HGG Advances

ARTICLE

X chromosome inactivation in the human placenta is patchy and distinct from adult tissues

Tanya N. Phung,[1,2] Kimberly C. Olney,[1,2] Brendan J. Pinto,[1,2,3] Michelle Silasi,[4] Lauren Perley,[5] Jane O'Bryan,[5] Harvey J. Kliman,[5] and Melissa A. Wilson[1,2,6,*]

Summary

In humans, one of the X chromosomes in genetic females is inactivated by a process called X chromosome inactivation (XCI). Variation in XCI across the placenta may contribute to observed sex differences and variability in pregnancy outcomes. However, XCI has predominantly been studied in human adult tissues. Here, we sequenced and analyzed DNA and RNA from two locations from 30 full-term pregnancies. Implementing an allele-specific approach to examine XCI, we report evidence that XCI in the human placenta is patchy, with large patches of either maternal or paternal X chromosomes inactivated. Further, using similar measurements, we show that this is in contrast to adult tissues, which generally exhibit mosaic X inactivation, where bulk samples exhibit both maternal and paternal X chromosome expression. Further, by comparing skewed samples in placenta and adult tissues, we identify genes that are uniquely inactivated or expressed in the placenta compared with adult tissues, highlighting the need for tissue-specific maps of XCI.

Introduction

X chromosome inactivation (XCI) evolved in therian mammals at the same time as the development of invasive placentation and is important for many biological processes.[1] XCI is a mechanism to regulate the dosage of gene expression due to the differences in the number of X chromosomes between the sexes: genetic females (XX) have two X chromosomes while genetic males (XY) have only one X chromosome.[2,3]

There are two levels of XCI. The first level is at the whole-chromosome level, where either the maternal X or the paternal X is chosen for inactivation. The choice of which X is inactivated has been observed to happen in one of two ways: random XCI (the maternal and paternal X are inactivated with equal probability) and imprinted XCI (the paternal X is inactivated). In mice, the extraembryonic lineages that ultimately give rise to the placenta and some extraembryonic membranes show paternally imprinted XCI.[4–6] Paternally imprinted XCI has also been reported in rats,[7] cows,[8] and marsupial mammals.[9–11] However, in mice, the embryonic lineages that ultimately give rise to the rest of the fetus exhibit random XCI.[4] Random XCI has also been reported in mule and horse placenta.[12]

The second level of XCI concerns which individual genes are subject to inactivation (silenced or not expressed) on the inactive X chromosome. Previous studies have aimed to determine what genes on the X chromosome escape XCI in a variety of tissues (see Carrel and Brown[13] for an overview of expression from the inactive X). Carrel and Willard[14] studied biallelic expression in primary human fibroblast cell lines and rodent and human somatic hybrids. Cotton et al.[15] used DNA methylation data to characterize escape status in 27 adult tissues. Gene-specific inactivation has also been shown to vary between tissues and individuals in mouse and human.[16,17] However, previous cross-tissue studies on gene-specific escape from XCI did not include the placenta.

The human placenta is a transient tissue that is formed early in pregnancy and develops from the outer layer of the pre-implantation embryos.[18,19] The placenta has the genotype of the fetus and plays a critical role in pregnancy by regulating nutrition and protecting the developing fetus from the pregnant person's immune system.[20] Improper placenta development can lead to complications, such as pre-eclampsia and fetal growth restriction.[21] It is important to study gene-specific escape in the placenta because XCI could play an important role in pregnancy complications. Gong et al.[22] found that the spermine synthase gene (SMS) that modulates fetal growth restriction, a common pregnancy complication, may escape XCI in the placenta, but not in other tissues. Further, the degree of XCI skewing could be associated with pregnancy loss.[23] Therefore, understanding XCI in this early formed tissue is critical for understanding downstream developmental effects.

Previous research suggests that XCI across the entire X chromosome in the placenta is random and patchy, but these studies relied on a limited number of loci and did not investigate chromosome-wide, gene-specific variability or compare with adult tissues.[24,25] Further, one of

[1]Center for Evolution and Medicine, Arizona State University, PO Box 874501, Tempe, AZ 85282, USA; [2]School of Life Sciences, Arizona State University, PO Box 874501, Tempe, AZ 85282, USA; [3]Department of Zoology, Milwaukee Public Museum, Milwaukee, WI 53233, USA; [4]Department of Maternal-Fetal Medicine, Mercy Hospital St. Louis, St. Louis, MO 63141, USA; [5]Department of Obstetrics, Gynecology and Reproductive Sciences, Yale University School of Medicine, New Haven, CT 06520, USA; [6]The Biodesign Center for Mechanisms of Evolution, Arizona State University, PO Box 874501, Tempe, AZ 85282, USA

*Correspondence: mwilsons@asu.edu

https://doi.org/10.1016/j.xhgg.2022.100121.

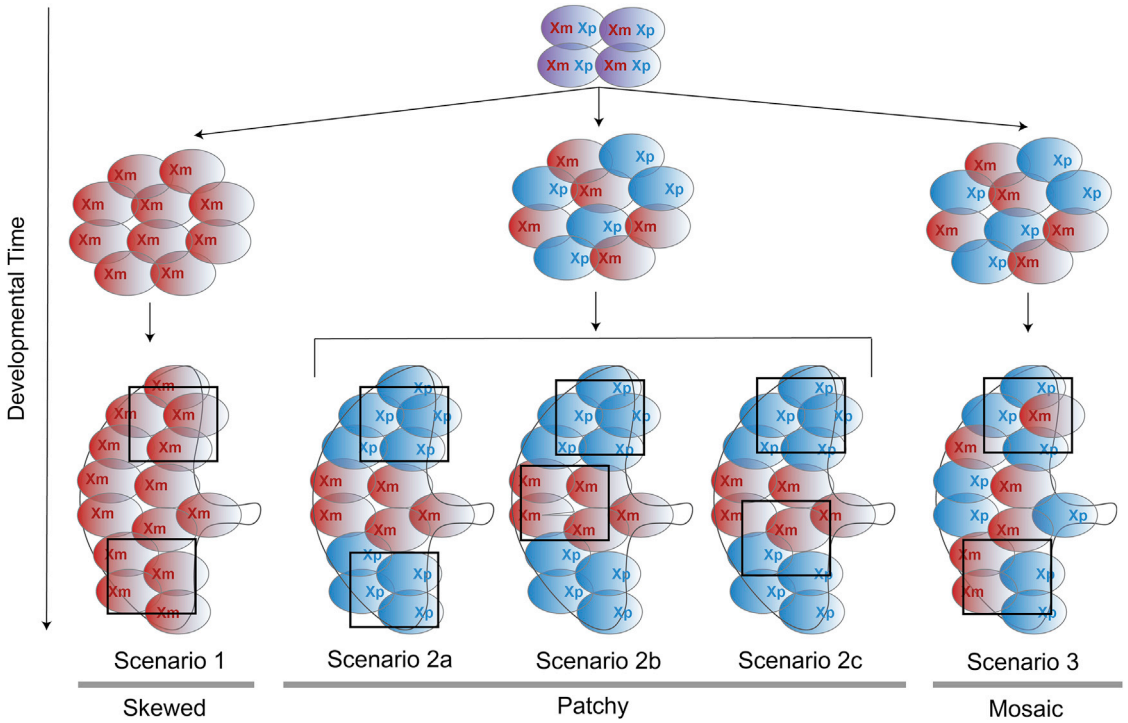

Figure 1. Schematic possible patterns of X chromosome inactivation
Prior to XCI, both the maternal and the paternal X chromosomes are present (purple cells). The blue cell represents the maternal X is inactivated, and the red cell represents the paternal X is inactivated. If XCI occurs very early in development and propagates to all daughter cells, we would observe extreme skewing, where all placentas show the same X inactivated. In this case, the same X chromosome is inactivated in both sites sampled from this study. If XCI occurs at an intermediate stage, XCI is random but is present with large patches of daughter cells with only the maternal X or paternal X. In this case, three possible scenarios can happen: (1) both of the sites sampled in this study happen to come from two patches with the same X inactivated, (2) each site sampled in this study comes from two patches with different X inactivation, and (3) one of the sites sampled in this study comes from the boundary of two patches. If XCI occurs very late in development, there are either small or no patches, creating a mosaic pattern of XCI.

the challenges of previous research on XCI is that indirect methods have been used to infer inactivation. Gong et al.[22] and Tukiainen et al.[17] used higher expression in females as compared with males as a proxy for escape genes, rather than directly measuring inactivation status. Slavney et al.[26] observed that escape genes tend to show higher expression compared with inactivated genes in both males and females but with little ability to discriminate between individual gene escape and inactivation, especially for heterogeneously escaping genes.

Here, we utilized next-generation sequencing to characterize genome-wide patterns of XCI in the human placenta. We further compared patterns of XCI between the placenta and adult tissues in humans and analyzed genes with an XCI status that is unique to the placenta. We studied allele-specific expression from 30 full-term placentas from uncomplicated pregnancies by performing whole-exome and whole-transcriptome (from two locations) sequencing, where the sex of the offspring was assigned female at birth. We further utilized data from the Genotype-Tissue Expression (GTEx) project to study and compare patterns of XCI in adult tissues.[27] Using our experimental approach, we have the capacity to observe (1) extreme skewing in the human placenta, where all placentas show the same X inactivated in both sites; (2) patchiness, where the placenta exhibits patches of daughter cells either maternal or paternal X expression only; or (3) mosaicism, where clusters of cells in a sample exhibit both maternal and paternal X chromosome expression (Figure 1). In this study, we limited analysis of gene-specific inactivation to placental and adult tissues with skewed XCI to directly measure allele-specific expression. We observed evidence for skewing (large patches of exclusively maternal or paternal X expression) in the human placenta that is not present in adult tissues. We also compared genes that are inactivated, genes that escape from inactivation, and genes that show variable escape between the placenta and adult tissues. While a majority of genes are concordant for inactivation status between the placenta and adult tissues (71%), we observed a subset of genes that show opposite patterns between the placenta and adult tissues.

Our results provide additional evidence that XCI in the human placenta is random and patchy. Our study further shows that patterns of X inactivation differ between embryonic tissue and adult tissues, consistent with different developmental structures of these tissues. Finally, we identified genes with unique XCI status in the placenta. We hypothesize that these genes could play an important role in the placenta and pregnancy.

Material and methods

Samples collection

Working with the Yale Biobank, we collected samples from 30 placentas, where the sex of the offspring was assigned female at birth. We confirmed that the samples were genetically XX by the presence of heterozygous sites across the X chromosome. The placenta samples were collected immediately following birth from term (≥36 weeks and 6 days) uncomplicated pregnancies delivered by cesarean section. Placentas were collected and sequenced at two different times, with 12 placenta samples in the first batch (OBG0044, OBG0068, OBG0111, OBG0115, OBG0120, OBG0133, OBG0156, OBG0170, OBG0174, OBG0175, OBG0178, and OBG0166) and 18 in the second (OBG0022, OBG0024, OBG0026, OBG0028, OBG0030, OBG0039, OBG0050, OBG0051, OBG0066, OBG0121, OBG0138, OBG0180, OBG0188, OBG0201, OBG0205, OBG0289, OBG0338, and OBG0342).

Placental tissue samples were obtained through rapid sampling (≤30 min post-delivery). Tissue samples were taken from the "maternal" side, midway between the chorionic and basal plates, from the periphery of the lobules, avoiding maternal tissue, consistent with best practices.[28] Sampling sites were free of visible infarction, calcification, hematoma, and tears (areas of frank visible pathology were avoided). Whenever possible, tissue samples were obtained from distinct cotyledons of the placenta in opposing quadrants of the placenta (far from one another spatially).

The sampling protocol was as follows:

1. Orient the placenta maternal side up (basal plate uppermost) and identify sampling areas in each of the four placental quadrants.
2. At each site, remove the basal plate (to remove maternal tissue) ~1 to 2 mm by trimming with a pair of sterile scissors to expose villous tissue.
3. Cut a "grape-sized" (approximately 1 to 2 cm^3; 5 to 6 g) tissue lobule from each of the four quadrants.
4. Wash the tissue thoroughly twice in phosphate-buffered saline (PBS) solution and blot on clean gauze.
5. From each grape-sized lobule, cut away eight smaller pieces (~1 to 2 mm^3) using a scalpel.
6. For each sampling quadrant, place four of the ~50-mg tissue pieces in a labeled cryovial. Snap freeze immediately in liquid nitrogen. Store samples at −80°C until ready for use; aliquot individual tissue pieces as needed per research protocols.
7. For each sampling quadrant, place four of the tissue pieces in a labeled cryovial containing 1 mL of RNAlater solution (RNA-stabilizing agent). Store the cryovials in the 4°C benchtop fridge for a minimum of 48 h, and a maximum of 7 days, per RNAlater manufacturer protocol. After a minimum of 48 h, use a pipette to remove the RNAlater solution from the cryovials and immediately snap freeze in liquid nitrogen. Store samples at −80°C until ready for use; aliquot individual tissue pieces as needed per research protocols.

Whole-exome sequencing

DNA was extracted from one flash-frozen collection site for each individual. Exome libraries were prepped and sequenced to approximately 50× coverage with 100-bp paired-end sequence on the Illumina NextSeq at the Yale Genome Sequence Center.

Whole-transcriptome sequencing

From each placenta, two separate sites from opposite quadrants were collected. RNA was extracted, and RiboZero stranded libraries (RF) were prepared and sequenced to approximately 40 million reads per sample with 100-bp paired-end sequence on the Illumina NovaSeq at the Yale Genome Sequence Center.

Exome sequence data processing

We used fastqc v.0.11.8[29] for quality control and aggregated results from fastqc by using multiqc v.0.9.[30] We trimmed adapters using bbduk as part of bbmap v.38.22.[31] Sequences were trimmed both left and right for phred quality of 30, minimum length of 75 bp, and average read quality of 20 or greater to keep only high-quality reads.[31] Quality was checked after trimming (Figure S1). We confirmed genetic XX females by examining the reads mapped ratio between the X chromosome and chromosome 19 (chrX/chr19), between the Y chromosome and chromosome 19 (chrY/chr19), and between the Y chromosome and the X chromosome (chrX/chrY). We observed that sample OBG0175 has a lower chrX/chr19 reads mapped ratio than other samples in this study (Figure S2). Therefore, we removed sample OBG0175 from further analyses. We used bwa-mem v.0.7.17[32] to map to a female-specific reference genome. Specifically, we mapped the exome samples to a sex chromosome complement informed reference genome in which the Y chromosome is hard masked (to avoid mismapping of X-linked reads to homologous regions on the Y chromosome in the XX samples). Mapping exome samples to a reference genome with the Y chromosome hard masked has been shown to increase the number of variants genotyped on the X chromosome.[33] To generate the sex chromosome complement reference genome, we employed XYalign.[33] XYalign created a Y-masked gencode GRCh38.p12 human reference genome for aligning XX individuals.[34] We used picard v.2.18.27[35] to mark PCR duplicates. To genotype variants, we used GATK v.4.1.0.0.[36–38] We first used GATK's HaplotypeCaller to generate GVCF files. Second, we combined GVCF from 66 samples using GATK's CombineGVCFs (30 placenta samples and an additional 36 samples from a separate study in the group [unpublished data] here to increase power to genotype variants). Finally, we used GATK's GenotypeGVCFs to call variants. Following GATK's best practice, we obtained high-quality variants by filtering using GATK's Variant Quality Score Recalibration (VQSR). We tabulated the number of heterozygous variants for each sample in Table S1. Because we sequenced the placenta samples in two separate batches, we plotted the principal component for the exome data using the package *SNPRelate* in R[39] and observed no separation by batch from the exome data (Figure S3).

Whole-transcriptome data processing

Samples were checked for quality using fastqc v.0.11.8,[29] and results were aggregated across samples using multiqc v.0.9.[30] Adapters were removed and sequences were trimmed both left and right for phred quality of 30, minimum length of 75 bp, and average read quality of 20 or greater using bbduck v.38.22.[31] Quality was checked after trimming (Figure S4). Trimmed RNA sequencing (RNA-seq) female placenta reads were then aligned to a sex chromosome complement informed reference genome with the Y chromosome hard masked with Ns[33,40] using the gencode GRCh38.p12 reference genome.[34] RNA-seq samples were aligned using HISAT2,[41] which has been shown to be a robust aligner for high-throughput RNA-seq reads. Total reads mapped

and duplicate reads were visually checked using BAMtools stats (Table S2).[42]

Obtaining allele counts for allele-specific expression analysis

We used GATK ASEReadCounter (v.4.1.0.0) to obtain allele counts[36] with the following thresholds: min-depth-of-non-filtered-base = 1, min-mapping-quality = 10, and min-base-quality = 10. GATK ASEReadCounter automatically filters out duplicated reads. Duplicated reads are suggested to be removed for allele-specific expression analysis.[43] The number of heterozygous and expressed variants for each sample are reported in Table S3.

GTEx data processing

We downloaded ASEReadCounter counts for the X chromosome and chromosome 8 from the GTEx project, approved for project no. 8834 for General Research Use in GTEx to M.A.W. We only considered tissues with more than 10 samples per tissue and excluded two non-primary tissues: Epstein-Barr virus (EBV)-transformed lymphocytes and cultured fibroblasts, leaving 45 tissues to be analyzed in this study. We list the GTEx tissues, the number of samples per tissue examined in this study, and the number of skewed samples per tissue in Table S4. Notably, the tissue size sampled for each tissue in the GTEx dataset was approximately equal to that of the placental tissue samples collected in this study, with GTEx requiring samples to be less than 4 mm in thickness. Length may have been longer, ranging from 5 to 10 mm in length and width, though it is difficult to discern from the Tissue Harvesting Work Instruction (https://gtexportal.org/home/samplingSitePage) whether this full aliquot was used for the sequencing experiments.

Computing unphased median allele balance

For each heterozygous and expressed variant, ASEReadCounter tabulates the number of reads (the count) for the reference allele and the alternate allele. The total read count is the sum of the read count of the reference allele and the read count of the alternate allele. We define the biased allele to be the allele with more read counts. For each heterozygous and expressed variant, the unphased allele balance is the ratio between the read count of the biased allele and the total read count. Then, for each sample, the median allele balance is calculated by computing the median unphased allele balance across all heterozygous and expressed variants.

Defining threshold for allele-specific expression

To determine the threshold for defining biased allele expression, we plotted the unphased allele balance across all variants for each individual for chromosome 8 and the X chromosome (Figure S5). We observed that the unphased allele balance of most variants on the X chromosome is greater than 0.8, while the unphased allele balance of most variants on chromosome 8 is less than 0.8 (Figure S5). Therefore, in this study, we used 0.8 as a threshold for biased allele-specific expression.

Determining which X chromosome is inactivated

At the whole X chromosome level, to determine whether the same X chromosome is inactivated at the two extraction sites for each placenta sample, we employed a phasing strategy on the X chromosome by defining that the biased alleles (the alleles with higher counts) are on the same haplotype. We restricted this analysis to contain only heterozygous and expressed variants that are shared between the two extraction sites. For consistency, we defined extraction site A to be the site with more expressed variants where the unphased allele balance is greater than 0.8. We defined the activated X chromosome to consist of alleles where its allele balance (the ratio between this allele's read count and the total read count) is greater than 0.8. In cases where the allele balance is less than 0.8, we picked an allele at random with equal probability between the reference allele and the alternate allele. Then, we computed the allele balance (defined as the ratio between the biased allele's count and total count) for the alleles on the same X chromosome. We called this phased allele balance. At each site, we computed the median phased allele balance to use as summary statistics. To compute phased allele balance, we followed this procedure:

1. Find expressed variants that are shared between site A and site B.
2. Using the shared expressed variants between site A and site B, tabulate the number of expressed variants that exhibit biased expression (i.e., unphased allele balance is greater than 0.8).
3. Pick a site to base phasing from based on the number of expressed variants with biased expression. For example, if site A has 50 expressed variants with biased expression and site B has 60 such variants, phasing is based on site B.
4. Phasing strategy (using site B to base phasing): the expressed haplotype is generated by the following calculation: For each expressed variant that is shared between site A and site B, pick the allele with allele balance greater than 0.8 to be on the expressed haplotype. If allele balance is less than 0.8, choose an allele at random with equal probability.

Validating method based on allele-specific expression to quantify XCI

We validated our approach to determine skewness by examining the non-pseudoautosomal regions (nonPARs) of the X chromosome in males. We collected samples from 12 placentas, where the sex of the offspring was assigned male at birth. Even though the X chromosome in males is haploid, some variants are incorrectly genotyped as being heterozygous when diploidy is assumed when genotyping with GATK (Table S5). Regardless, these heterozygous variants exhibit mostly skewed expression, indicating that our method of combining both the whole-exome and whole-transcriptome sequence data is robust to determine skewness (Figure S6).

Classifying genes into genes that are inactivated, genes that escape XCI, and genes that show variable escape

At the per-gene level, we only considered samples that show skewed expression (allele balance is greater than 0.8). There are 52/58 samples in the placenta dataset and 525/4,958 samples in the GTEx dataset exhibiting skewed expression that were used for this analysis. For each gene on the X chromosome, we only considered a gene if there were at least five informative samples where in each sample there is at least one heterozygous and expressed variant for that gene. If there are more than one heterozygous and expressed variant for a gene, we summed up the counts

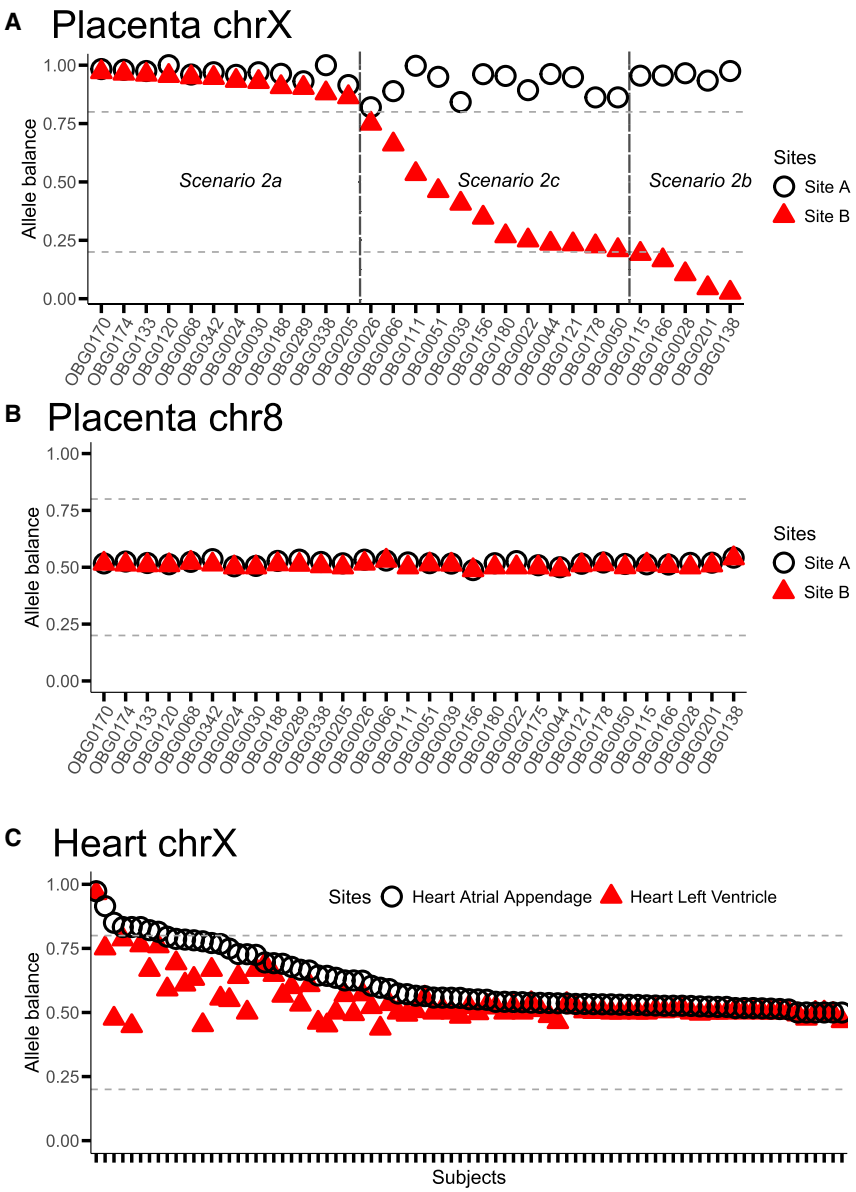

Figure 2. X chromosome inactivation is patchy in the human placenta and mosaic in the human heart

Phased allele balance aggregated across variants for each sample is shown for site A (open black circle) and site B (filled red triangle). Each point is the median value across variants. Median was used to minimize the effect of outliers. The dotted gray horizontal lines denote allele balance of 0.2 and 0.8.

(A) Placenta X chromosome. We removed variants that fall within the pseudoautosomal regions (PARs) prior to computing medians.

(B) Placenta chromosome 8.

(C) Heart X chromosome.

for the biased allele and calculated allele balance by dividing the summed counts of the biased allele by the summed counts of the total counts. We categorized a gene as being inactivated if its allele balance is greater or equal to 0.8 in at least 70% of the samples and the median allele balance across all samples is greater or equal to 0.8. We categorized a gene as escaping from XCI if at most 30% of the samples have allele balance for this gene $\geq$0.8 and the median allele balance across all samples is $\leq$0.75. Otherwise, the gene is annotated as showing variable escape across all individuals. See Note S1 for more information on gene categorization and Table S6 for status of specific genes.

Coordinates used of PARs and XIST

As defined for GRCh38.p12,[44] we used the following coordinates for the pseudoautosomal region 1 (PAR1), PAR2, and XIST:

PAR1: position 10,001 to position 2,781,479 on the X chromosome

PAR2: position 155,701,383 to position 156,030,895 on the X chromosome

XIST: position 73,820,651 to position 73,852,723 on the X chromosome

Results

Whole-chromosome level of X chromosome inactivation differs between the placenta and adult tissues

We observed evidence for patchiness in XCI in the placenta. To examine patterns of XCI in the human placenta, we sequenced the whole transcriptome from two separate extraction sites of the same placenta. We then employed a phasing strategy on the X chromosome using whole-exome and whole-transcriptome sequence data. Briefly, at heterozygous sites that exhibit allelic imbalance, we reasoned that the biased alleles (the alleles that are expressed in a higher proportion) are all on the same X chromosome (see material and methods). In 17/29 placentas, both sites in the placenta exhibited extremely skewed X inactivation, either with both extraction sites showing the same inactivated X chromosome (12 placentas; Figures 2A and S7A) or each site showing the opposite X chromosome inactivated (five placentas; Figures 2A and S7B). In the remaining 12 placentas, we observed one extraction site showing skewed XCI and the other showing variable proportions of both X chromosomes being expressed (Figures 2A and S7C). In this subset, we postulated that one of our samples was collected on the boundary of two different patches of X inactivated cells. To validate that the patterns we observed on the X chromosome are indeed XCI, we repeated the same analyses on chromosome 8, where all samples showed biallelic expression (Figure 2B). Our results suggest that the human placenta is organized into large patches with either the maternal or paternal X chromosome being inactivated.

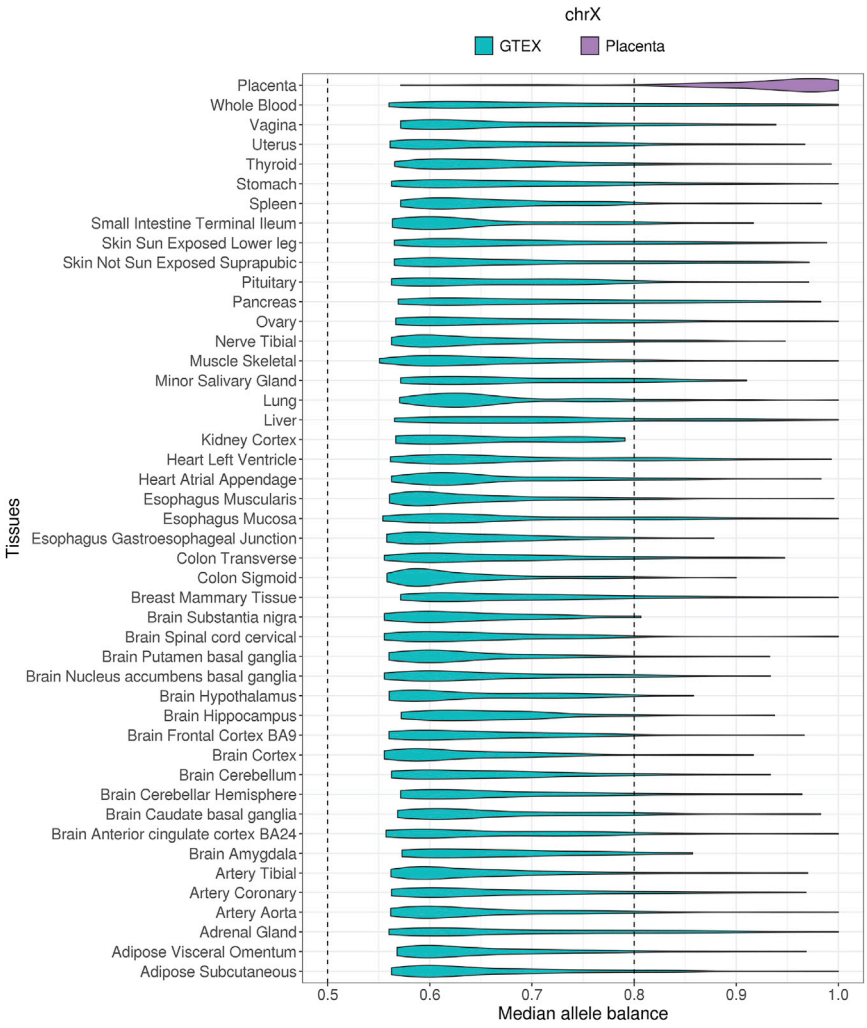

Figure 3. Whole chromosome level of X chromosome inactivation differs between the placenta and adult tissues in humans

Unphased median allele balance is plotted for the placenta in this study (purple) and for 45 adult tissues in the GTEx dataset (blue). Each point of the violin plot is the median allele balance for each sample. Because there are no multiple site samplings for the GTEx data, unphased allele balance was computed. Here, the pseudoautosomal regions of the X chromosome are removed.

We found that patterns XCI in the placenta are different from adult tissues (Figures 2 and 3). We first compared the pattern of whole-chromosome XCI in the two placenta samples we collected with whole-chromosome XCI in two regions collected from adult human hearts (left ventricle and atrial appendages) sampled by the GTEx consortium (Figures 2A and 2C).[27] We identified 85 individuals with RNA-seq data for both of these locations in the heart and employed the same phasing approach as in the placenta. In the heart tissue, both regions exhibit biallelic expression (both maternal and paternal X expression) in 91% of individuals (Figure 2C). This is in stark contrast to the placenta, where none of individuals exhibit biallelic expression at both regions (Figure 2A).

We further found the same biallelic pattern of XCI across all 43 adult tissue samples, in contrast to the placenta (Figure 3). Because other adult tissues include a single sample,[27] to assess chromosome-wide XCI, we compared median allele balance computed from the biased allele for each sample. While most placenta samples (90%) exhibit skewed allele balance (i.e., allele balance greater than 0.8), most samples from adult tissues (89%) exhibit biallelic expression (i.e., allele balance between 0.5 and 0.8) (Figure 3). Similar to the placenta, however, also we observed biallelic expression across all adult tissues on chromosome 8, as expected (Figure S8). Together, these results suggest that patterns of whole-chromosome XCI differ between the placenta and adult tissues.

Gene-specific escape comparison between the placenta and adult tissues

We observed a large degree of variability in gene-specific escape in the placenta, both across and within individuals. We categorized genes on the X chromosome using only samples that exhibit skewed median allele balance across the X chromosome (i.e., median allele balance greater than 0.8; see material and methods). Only seven genes (4%) show evidence for escape across all samples with the ability to assay, while 73 genes (37%) show evidence of inactivation across all samples (Figure S9). Rather, most genes, 116 genes (59%), show a gradient of the proportion of samples that exhibit evidence for escape. In addition, heterogeneity exists between two sites within individuals (Figure S10). Given the tremendous heterogeneity in evidence for escape, we additionally investigated the ratio of female-to-male gene expression across X-linked genes. We observed that genes in all three classes (escape, variable, and inactivated) exhibit a range of female-to-male gene expression ratios, with higher gene expression in females as compared with males underpowered to determine whether a gene has escaped X inactivation (Figure S11).

We found similarities and differences in gene-specific escape and inactivation in the human placenta when compared with the adult tissues. We used 525 skewed adult tissue samples in the GTEx dataset (out of 4,958 total samples) and 52 skewed samples in the placenta dataset (out of 58 total samples) to categorize XCI status (see material and methods). A gene is considered for this analysis if there are at least five informative samples (i.e., an informative

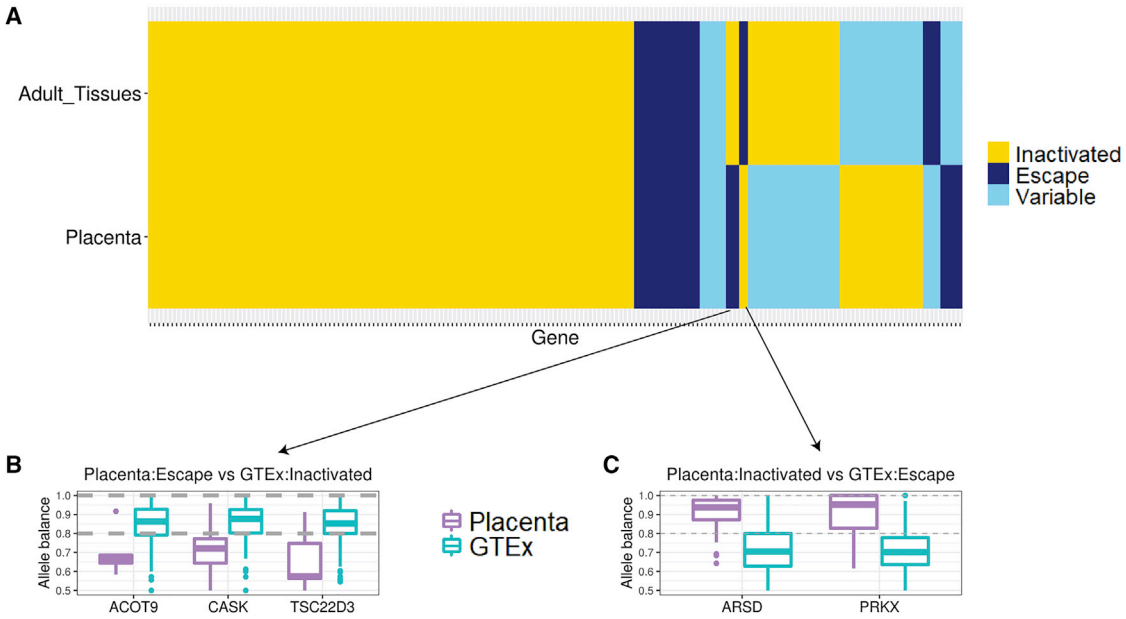

Figure 4. Gene-specific escape comparison between the placenta and adult tissues

(A) A heatmap showing genes that are inactivated in both the placenta and adult GTEx tissues (yellow), genes that escape X chromosome inactivation in both the placenta and adult GTEx tissues (dark blue), and genes that exhibit variable escape across individuals in both the placenta and adult GTEx tissues (light blue).

(B and C) Boxplots showing median allele balance across all samples in the placenta (purple) and adult tissues in GTEx (blue) for the three genes that show evidence for escaping XCI in the placenta but being inactivated in the adult GTEx tissues (B) and for the two genes that show evidence for being inactivated in the placenta but escaping in the adult GTEx tissues (C). Each point of the box plot is the median allele balance computed across variants for that gene (see material and methods).

sample is defined as having at least one heterozygous and expressed variant for that gene) in both the placenta dataset and the GTEx dataset. We found 186 such genes. Out of these 186 genes, 132 genes (71%) show the same pattern of escape or inactivation between the adult tissues and the placenta dataset (Figure 4A). Specifically, 111 genes are inactivated, 15 genes escape, and 6 genes show variable escape between the adult tissues and the placenta. We also observed differences between the adult tissues and the placenta. We found three genes that escape in the placenta but are inactivated in adult tissues: *ACOT9*, *CASK*, and *TSC22D3* (Figure 4B). We found two genes that are inactivated in the placenta but escape in adult tissues: *ARSD* and *PRKX* (Figure 4C). We examined the mapping quality and total RNA read counts of the variants in these genes to confirm that these observations are not artifacts (Figure S12). These results suggest that, while the majority of genes on the X chromosome show consistent XCI between the placenta and adult tissues, a subset exhibits opposite patterns that could be attributed to the unique nature of the placenta tissue, which is an embryonic tissue.

Finally, for a subset of our placenta samples, we also had access to maternal exome samples and used these to assess whether the silenced sample was maternal or paternal in origin and observed that most inactivated X chromosomes were paternal in origin (Table S7). In 18/30 placentas, we also sequenced the whole exome of the decidua, allowing us to determine whether the maternal or paternal X chromosome is inactivated (see material and methods). In 8/18 placenta samples where both extraction sites show the same inactivated X chromosome, it is the paternal X that is silenced in both (Table S7). In 3/18 placenta samples where one extraction site shows skewed X inactivation while the other extraction site shows both X chromosomes being expressed, in two of these cases, the paternal X is silenced (Table S7). In 7/18 placenta samples the two extraction sites necessarily show the opposite X chromosome being activated, either maternal or paternal (Table S7).

Discussion

We observed that XCI in the human placenta is organized into large patches of maternal or paternal X expression. We utilized whole-exome and whole-transcriptome sequence data to analyze allele-specific expression across female placentas and found evidence that the human placenta exhibits large patches of maternal or paternal X chromosome expression. While patchy XCI in the human placenta has been observed in humans previously, these prior studies rely on a few SNPs and a few genes in a limited number of samples.[24,45] For example, Looijenga et al.[45] examined two samples from each of the nine female (46, XX) full-term placenta samples, using methylation in a single gene, androgen receptor, as a readout, they found that three placentas exhibited predominantly maternal X inactivation, one exhibited paternal X inactivation, and the

remaining five exhibited both maternal and paternal alleles. In a different study, with at least five informative SNPs used to infer X inactivation status in a single site collected from 22 placentas, the authors similarly observe some placentas have maternal X inactivation, some have paternal X inactivation, and others show biallelic expression across the X-linked SNPs.[24] From this, the authors proposed that the human placenta has large patches of maternal or paternal X inactivation. These studies typically relied on a single gene, as in Looijenga et al.,[45] or when these studies did not include multiple samplings from the same placenta, the number of samples is small (i.e., three) as in Moreira de Mello et al.[24] With improved sampling (i.e., sampling two independent locations from each placenta, from opposing quadrants) and genome-wide sequencing, we confirm that patterns of XCI are predominantly patchy in the human placenta.

We found distinct patterns of XCI between the placenta and adult tissues in humans: while most placenta samples (~90%) exhibit skewed expression, only about 11% of samples from human adult tissues exhibit skewed expression. This is consistent with previous methylation-based analyses that observed skewed inactivation across different developmental layers of the placenta,[25] suggesting that each villus tree is clonally derived from a few precursor cells and that there is little cell migration across placental regions. This is in contrast to adult tissues, where we observe very little skewing, suggesting more cell migration during development, though both observations are contingent on the size of the tissue sample analyzed in bulk, where samples with more cells are more likely to capture both X chromosomes being expressed. Per our reading of the sample collection in GTEx (see material and methods), the bulk sample sizes were approximately the same size at collection (aiming for 10 mm × 10 mm × 4 mm) compared with the placenta samples collected here (10–20 mm cubed); however, it is not clear what size of this sample was sequenced by GTEx, compared with what was sequenced here (2 mm cubed was sequenced per placenta sample). It is possible that a larger bulk sample was sequenced by the GTEx consortium, resulting in the signal for biallelic expression across most adult tissues.

Although we found high concordance in genes that are inactivated and genes that escape between the placenta samples and adult tissues (Figure 4), we found a subset of genes with unique XCI status in the placenta. Specifically, we found five genes that show patterns that are unique to the placenta: *ACOT9*, *CASK*, and *TSC22D3* are inactivated in adult tissues but escape XCI in the placenta (Figure 4B). *ACOT9* has been associated with syndromic X-linked intellectual disability Turner Type,[46] but the function of *ACOT9* in the placenta is unclear. *CASK* is critical in brain development post-natally,[47] as well as prenatal brain development in both males and females, but with varying phenotypes,[48] potentially due to its escape from inactivation (biallelic expression) in females compared with males. *TSC22D3* is an immunity-related gene. Syrett al.[49] observed that *TSC22D3* is overexpressed in females compared with males in T cells of patients with systemic lupus erythematosus. In contrast to the previous three genes, *ARSD* and *PRKX*, both genes in the pseudoautosomal region, escape XCI in adult tissues but are inactivated consistently across regions in the placenta (Figure 4C). Larson et al.[50] observed that *ARSD* is inactivated in at least one ovarian tumor sample, highlighting a potential parallel between the placenta and tumor development.[50] *PRKX* has been previously reported to escape in adult fibroblasts and lymphoblasts.[51] Curiously, PRKX is also involved in fetal kidney development,[52] and so perhaps its silencing is important for dosage during development, but further studies are needed to determine whether there are sex differences in *PRKX* expression in the placenta. We hypothesize that these five genes could be further studied for a potential role in pregnancy and pregnancy complications.

We additionally show that sex differences in gene expression are not sufficient on their own to determine whether a gene escapes inactivation or not (Figure S11). This highlights the importance of understanding both inactivation status and expression differences between the sexes. Gong et al.[22] used female-biased gene expression as a proxy for identifying potential genes that escape XCI in the placenta. Twenty-eight of forty-seven potential escape genes identified by Gong et al.[22] were reported previously as being inactivated or unknown. Of these, 3/28 genes exhibit variable escape in our placenta data (*MBTPS2*, *SMS*, and *PIN4*) and only 1/28 genes exhibit evidence for escaping (*CXorf36*). This means the other 24/28 show female-biased expression but no evidence of escape in the placenta. Thus, it will be critical for studies interested in studying XCI to assess allele-specific expression explicitly.

There has also been interest in whether the maternal or paternal X chromosome is preferentially inactivated. In mice, the paternal X is preferentially inactivated in extra-embryonic tissues,[53] potentially due to unique methylation of XIST in sperm compared with eggs resulting.[54] Further, the paternal X is preferentially inactivated in rat yolk sac.[7] However, as we show here, approximately half of our samples show patchiness of XCI, with both parents' X chromosomes being expressed in one quadrant or the other. This is consistent with observed randomness of X inactivation in the placenta in horses as well.[12] That said, for the subset of samples where only one parent's X chromosome is expressed in both quadrants, we curiously observe that, overwhelmingly, it is the paternal X chromosome that is inactivated.

Future work should also focus on confirming whether certain genes that show a variable pattern of inactivation across the two quadrants studied here are indeed variable using spatial transcriptomic or single-cell analyses. Single-cell data for the placenta have been generated (e.g., Pique-Regi et al.,[55] Vento-Tormo et al.,[56] and Ashary et al.[57]) that could potentially be used for future analyses of this inactivation heterogeneity. Unfortunately, the

samples used in this study were collected in a manner inconsistent with using them for single-cell isolation.

In conclusion, we confirmed that XCI in the human placenta is skewed but patchy and conducted allele-specific expression analyses in adult tissues to show that, in contrast to the placenta, most adult samples show mosaic inactivation in bulk samples. Using the subset of adult tissues that do show skewed inactivation, we identified a subset of genes showing patterns of XCI that are unique to the placenta that should be further investigated for their roles in pregnancy and placentation. We further report that sex differences in expression are not sufficient to predict X inactivation and that, where there is bias (only one parent's X chromosome being inactivated across the two samples), this tends to be the parental X chromosome.

Data and code availability

The datasets generated during this study are available via controlled access: phs002240.v1.p1 NIGMS Sex Differences Placentas. The code generated during this study is available at https://github.com/SexChrLab/Placenta_XCI.

Supplemental information

Supplemental information can be found online at https://doi.org/10.1016/j.xhgg.2022.100121.

Acknowledgments

We acknowledge Research Computing at Arizona State University for providing high-performance computing and storage resources that have contributed to the research results reported within this paper (http://www.researchcomputing.asu.edu). We would also like to thank Heini Natri and Wilson lab members for helpful feedback on the manuscript. This work was supported by the National Institute of General Medical Sciences (NIGMS) of the National Institutes of Health grant R35GM124827 to M.A.W. This research was supported by The Yale University Reproductive Sciences Data and Specimen Biorepository, HIC#1309012696, a component of the Department of Obstetrics, Gynecology & Reproductive Sciences, Yale School of Medicine, New Haven, CT. Research reported in this publication was supported by the Eunice Kennedy Shriver National Institute Of Child Health & Human Development of the National Institutes of Health under award number F31HD101252 to K.C.O. K.C.O. was additionally supported by ARCS Spetzler Scholar.

Declaration of interests

The authors declare no competing interests.

Received: January 18, 2022
Accepted: May 16, 2022

References

1. Natri, H., Garcia, A.R., Buetow, K.H., Trumble, B.C., and Wilson, M.A. (2019). The pregnancy pickle: evolved immune compensation due to pregnancy underlies sex differences in human diseases. Trends Genet. *35*, 478–488. https://doi.org/10.1016/j.tig.2019.04.008.
2. Lyon, M.F. (1961). Gene action in the X-chromosome of the mouse (Mus musculus L.). Nature *190*, 372–373. https://doi.org/10.1038/190372a0.
3. Wilson Sayres, M.A., and Makova, K.D. (2013). Gene survival and death on the human Y chromosome. Mol. Biol. Evol. *30*, 781–787. https://doi.org/10.1093/molbev/mss267.
4. Takagi, N., and Sasaki, M. (1975). Preferential inactivation of the paternally derived X chromosome in the extraembryonic membranes of the mouse. Nature *256*, 640–642. https://doi.org/10.1038/256640a0.
5. Huynh, K.D., and Lee, J.T. (2001). Imprinted X inactivation in eutherians: a model of gametic execution and zygotic relaxation. Curr. Opin. Cell Biol. *13*, 690–697. https://doi.org/10.1016/s0955-0674(00)00272-6.
6. Huynh, K.D., and Lee, J.T. (2005). X-chromosome inactivation: a hypothesis linking ontogeny and phylogeny. Nat. Rev. Genet. *6*, 410–418. https://doi.org/10.1038/nrg1604.
7. Wake, N., Takagi, N., and Sasaki, M. (1976). Non-random inactivation of X chromosome in the rat yolk sac. Nature *262*, 580–581. https://doi.org/10.1038/262580a0.
8. Xue, F., Tian, X.C., Du, F., Kubota, C., Taneja, M., Dinnyes, A., Dai, Y., Levine, H., Pereira, L.V., and Yang, X. (2002). Aberrant patterns of X chromosome inactivation in bovine clones. Nat. Genet. *31*, 216–220. https://doi.org/10.1038/ng900.
9. Richardson, B.J., Czuppon, A.B., and Sharman, G.B. (1971). Inheritance of glucose-6-phosphate dehydrogenase variation in kangaroos. Nat. New Biol. *230*, 154–155. https://doi.org/10.1038/newbio230154a0.
10. Cooper, D.W., Johnston, P.G., Vandeberg, J.L., and Robinson, E.S. (1989). X-chromosome inactivation in marsupials. Aust. J. Zool. *37*, 411–417. https://doi.org/10.1071/zo9890411.
11. Al Nadaf, S., Waters, P.D., Koina, E., Deakin, J.E., Jordan, K.S., and Graves, J.A. (2010). Activity map of the tammar X chromosome shows that marsupial X inactivation is incomplete and escape is stochastic. Genome Biol. *11*, R122. https://doi.org/10.1186/gb-2010-11-12-r122.
12. Wang, X., Miller, D.C., Clark, A.G., and Antczak, D.F. (2012). Random X inactivation in the mule and horse placenta. Genome Res. *22*, 1855–1863. https://doi.org/10.1101/gr.138487.112.
13. Carrel, L., and Brown, C.J. (2017). When the Lyon(ized chromosome) roars: ongoing expression from an inactive X chromosome. Philos. Trans. R. Soc. Lond. B Biol. Sci. *372*, 20160355. https://doi.org/10.1098/rstb.2016.0355.
14. Carrel, L., and Willard, H.F. (2005). X-inactivation profile reveals extensive variability in X-linked gene expression in females. Nature *434*, 400–404. https://doi.org/10.1038/nature03479.
15. Cotton, A.M., Price, E.M., Jones, M.J., Balaton, B.P., Kobor, M.S., and Brown, C.J. (2015). Landscape of DNA methylation on the X chromosome reflects CpG density, functional chromatin state and X-chromosome inactivation. Hum. Mol. Genet. *24*, 1528–1539. https://doi.org/10.1093/hmg/ddu564.
16. Berletch, J.B., Ma, W., Yang, F., Shendure, J., Noble, W.S., Disteche, C.M., and Deng, X. (2015). Escape from X inactivation varies in mouse tissues. PLoS Genet. *11*, e1005079. https://doi.org/10.1371/journal.pgen.1005079.
17. Tukiainen, T., Villani, A.-C., Yen, A., Rivas, M.A., Marshall, J.L., Satija, R., Aguirre, M., Gauthier, L., Fleharty, M., Kirby, A., et al. (2017). Landscape of X chromosome inactivation across

human tissues. Nature *550*, 244–248. https://doi.org/10.1038/nature24265.
18. James, J.L., Carter, A.M., and Chamley, L.W. (2012). Human placentation from nidation to 5 weeks of gestation. Part I: what do we know about formative placental development following implantation? Placenta *33*, 327–334. https://doi.org/10.1016/j.placenta.2012.01.020.
19. Turco, M.Y., and Moffett, A. (2019). Development of the human placenta. Development *146*, dev163428. https://doi.org/10.1242/dev.163428.
20. Gude, N.M., Roberts, C.T., Kalionis, B., and King, R.G. (2004). Growth and function of the normal human placenta. Thromb. Res. *114*, 397–407. https://doi.org/10.1016/j.thromres.2004.06.038.
21. Rathbun, K.M., and Hildebrand, J.P. (2019). Placenta abnormalities. In StatPearls (StatPearls Publishing).
22. Gong, S., Sovio, U., Aye, I.L., Gaccioli, F., Dopierala, J., Johnson, M.D., Wood, A.M., Cook, E., Jenkins, B.J., Koulman, A., et al. (2018). Placental polyamine metabolism differs by fetal sex, fetal growth restriction, and preeclampsia. JCI Insight *3*. https://doi.org/10.1172/jci.insight.120723.
23. Sui, Y., Chen, Q., and Sun, X. (2015). Association of skewed X chromosome inactivation and idiopathic recurrent spontaneous abortion: a systematic review and meta-analysis. Reprod. Biomed. Online *31*, 140–148. https://doi.org/10.1016/j.rbmo.2015.05.007.
24. Moreira de Mello, J.C., Araújo, É.S. S.d., Stabellini, R., Fraga, A.M., Souza, J.E. S.d., Sumita, D.R., Camargo, A.A., and Pereira, L.V. (2010). Random X inactivation and extensive mosaicism in human placenta revealed by analysis of allele-specific gene expression along the X chromosome. PLoS One *5*, e10947. https://doi.org/10.1371/journal.pone.0010947.
25. Peñaherrera, M.S., Jiang, R., Avila, L., Yuen, R.K.C., Brown, C.J., and Robinson, W.P. (2012). Patterns of placental development evaluated by X chromosome inactivation profiling provide a basis to evaluate the origin of epigenetic variation. Hum. Reprod. *27*, 1745–1753. https://doi.org/10.1093/humrep/des072.
26. Slavney, A., Arbiza, L., Clark, A.G., and Keinan, A. (2016). Strong constraint on human genes escaping X-inactivation is modulated by their expression level and breadth in both sexes. Mol. Biol. Evol. *33*, 384–393. https://doi.org/10.1093/molbev/msv225.
27. GTEx Consortium (2020). The GTEx Consortium atlas of genetic regulatory effects across human tissues. Science *369*, 1318–1330. https://doi.org/10.1126/science.aaz1776.
28. Konwar, C., Del Gobbo, G., Yuan, V., and Robinson, W.P. (2019). Considerations when processing and interpreting genomics data of the placenta. Placenta *84*, 57–62. https://doi.org/10.1016/j.placenta.2019.01.006.
29. Andrews, S. (2010). FastQC: a quality control tool for high throughput sequence data. Available online.
30. Ewels, P., Magnusson, M., Lundin, S., and Käller, M. (2016). MultiQC: summarize analysis results for multiple tools and samples in a single report. Bioinformatics *32*, 3047–3048. https://doi.org/10.1093/bioinformatics/btw354.
31. Bushnell, B. (2014). BBMap: A Fast, Accurate, Splice-Aware Aligner (Lawrence Berkeley National Lab. (LBNL)).
32. Li, H. (2013). Aligning Sequence Reads, Clone Sequences and Assembly Contigs with BWA-MEM. Arxiv. https://doi.org/10.48550/arXiv.1303.3997.
33. Webster, T.H., Couse, M., Grande, B.M., Karlins, E., Phung, T.N., Richmond, P.A., Whitford, W., and Wilson, M.A. (2019). Identifying, understanding, and correcting technical artifacts on the sex chromosomes in next-generation sequencing data. GigaScience *8*, giz074. https://doi.org/10.1093/gigascience/giz074.
34. Harrow, J., Frankish, A., Gonzalez, J.M., Tapanari, E., Diekhans, M., Kokocinski, F., Aken, B.L., Barrell, D., Zadissa, A., Searle, S., et al. (2012). GENCODE: the reference human genome annotation for the ENCODE Project. Genome Res. *22*, 1760–1774. https://doi.org/10.1101/gr.135350.111.
35. Picard Tools - By Broad Institute. http://broadinstitute.github.io/picard/
36. McKenna, A., Hanna, M., Banks, E., Sivachenko, A., Cibulskis, K., Kernytsky, A., Garimella, K., Altshuler, D., Gabriel, S., Daly, M., and DePristo, M.A. (2010). The Genome Analysis Toolkit: a MapReduce framework for analyzing next-generation DNA sequencing data. Genome Res. *20*, 1297–1303. https://doi.org/10.1101/gr.107524.110.
37. DePristo, M.A., Banks, E., Poplin, R., Garimella, K.V., Maguire, J.R., Hartl, C., Philippakis, A.A., del Angel, G., Rivas, M.A., Hanna, M., et al. (2011). A framework for variation discovery and genotyping using next-generation DNA sequencing data. Nat. Genet. *43*, 491–498. https://doi.org/10.1038/ng.806.
38. Van der Auwera, G.A., Carneiro, M.O., Hartl, C., Poplin, R., Del Angel, G., Levy-Moonshine, A., Jordan, T., Shakir, K., Roazen, D., Thibault, J., et al. (2013). From FastQ data to high confidence variant calls: the Genome Analysis Toolkit best practices pipeline. Curr. Protoc. Bioinformatics *43*, 11. https://doi.org/10.1002/0471250953.bi1110s43.
39. Zheng, X., Levine, D., Shen, J., Gogarten, S.M., Laurie, C., and Weir, B.S. (2012). A high-performance computing toolset for relatedness and principal component analysis of SNP data. Bioinformatics *28*, 3326–3328. https://doi.org/10.1093/bioinformatics/bts606.
40. Olney, K.C., Brotman, S.M., Valverde-Vesling, V., Andrews, J., and Wilson, M.A. (2020). Aligning RNA-Seq reads to a sex chromosome complement informed reference genome increases ability to detect sex differences in gene expression. Biol. Sex Differ. *11*, 42. https://doi.org/10.1186/s13293-020-00312-9.
41. Kim, D., Langmead, B., and Salzberg, S. (2015). HISAT: a fast spliced aligner with low memory requirements. Nat. Methods *12*, 357–360. https://doi.org/10.1038/nmeth.3317.
42. Barnett, D.W., Garrison, E.K., Quinlan, A.R., Strömberg, M.P., and Marth, G.T. (2011). BamTools: a C++ API and toolkit for analyzing and managing BAM files. Bioinformatics *27*, 1691–1692. https://doi.org/10.1093/bioinformatics/btr174.
43. Castel, S.E., Levy-Moonshine, A., Mohammadi, P., Banks, E., and Lappalainen, T. (2015). Tools and best practices for data processing in allelic expression analysis. Genome Biol. *16*, 195. https://doi.org/10.1186/s13059-015-0762-6.
44. Human Genome Overview - Genome Reference Consortium.
45. Looijenga, L.H., Gillis, A.J., Verkerk, A.J., van Putten, W.L., and Oosterhuis, J.W. (1999). Heterogeneous X inactivation in trophoblastic cells of human full-term female placentas. Am. J. Hum. Genet. *64*, 1445–1452. https://doi.org/10.1086/302382.
46. Stelzer, G., Rosen, N., Plaschkes, I., Zimmerman, S., Twik, M., Fishilevich, S., Stein, T.I., Nudel, R., Lieder, I., Mazor, Y., et al. (2016). The GeneCards suite: from gene data mining to disease genome sequence analyses. Curr. Protoc. Bioinformatics *54*, 1–30. https://doi.org/10.1002/cpbi.5.

47. Srivastava, S., McMillan, R., Willis, J., Clark, H., Chavan, V., Liang, C., Zhang, H., Hulver, M., and Mukherjee, K. (2016). X-linked intellectual disability gene CASK regulates postnatal brain growth in a non-cell autonomous manner. Acta Neuropathol. Commun. *4*, 30. https://doi.org/10.1186/s40478-016-0295-6.
48. Moog, U., Bierhals, T., Brand, K., Bautsch, J., Biskup, S., Brune, T., Denecke, J., de Die-Smulders, C.E., Evers, C., Hempel, M., et al. (2015). Phenotypic and molecular insights into CASK-related disorders in males. Orphanet J. Rare Dis. *10*, 44. https://doi.org/10.1186/s13023-015-0256-3.
49. Syrett, C.M., Paneru, B., Sandoval-Heglund, D., Wang, J., Banerjee, S., Sindhava, V., Behrens, E.M., Atchison, M., and Anguera, M.C. (2019). Altered X-chromosome inactivation in T cells may promote sex-biased autoimmune diseases. JCI Insight *4*, e126751. https://doi.org/10.1172/jci.insight.126751.
50. Larson, N.B., Fogarty, Z.C., Larson, M.C., Kalli, K.R., Lawrenson, K., Gayther, S., Fridley, B.L., Goode, E.L., and Winham, S.J. (2017). An integrative approach to assess X-chromosome inactivation using allele-specific expression with applications to epithelial ovarian cancer. Genet. Epidemiol. *41*, 898–914. https://doi.org/10.1002/gepi.22091.
51. Wainer Katsir, K., and Linial, M. (2019). Human genes escaping X-inactivation revealed by single cell expression data. BMC Genom. *20*, 201. https://doi.org/10.1186/s12864-019-5507-6.
52. Li, X., Li, H.-P., Amsler, K., Hyink, D., Wilson, P.D., and Burrow, C.R. (2002). PRKX, a phylogenetically and functionally distinct cAMP-dependent protein kinase, activates renal epithelial cell migration and morphogenesis. Proc. Natl. Acad. Sci. U. S. A. *99*, 9260–9265. https://doi.org/10.1073/pnas.132051799.
53. Harper, M.I., Fosten, M., and Monk, M. (1982). Preferential paternal X inactivation in extraembryonic tissues of early mouse embryos. J. Embryol. Exp. Morphol. *67*, 127–135. https://doi.org/10.1242/dev.67.1.127.
54. Zuccotti, M., and Monk, M. (1995). Methylation of the mouse Xist gene in sperm and eggs correlates with imprinted Xist expression and paternal X-inactivation. Nat. Genet. *9*, 316–320. https://doi.org/10.1038/ng0395-316.
55. Pique-Regi, R., Romero, R., Tarca, A.L., Sendler, E.D., Xu, Y., Garcia-Flores, V., Leng, Y., Luca, F., Hassan, S.S., and Gomez-Lopez, N. (2019). Single cell transcriptional signatures of the human placenta in term and preterm parturition. Elife *8*, e52004. https://doi.org/10.7554/elife.52004.
56. Vento-Tormo, R., Efremova, M., Botting, R.A., Turco, M.Y., Vento-Tormo, M., Meyer, K.B., Park, J.-E., Stephenson, E., Polański, K., Goncalves, A., et al. (2018). Single-cell reconstruction of the early maternal-fetal interface in humans. Nature *563*, 347–353. https://doi.org/10.1038/s41586-018-0698-6.
57. Ashary, N., Bhide, A., Chakraborty, P., Colaco, S., Mishra, A., Chhabria, K., Jolly, M.K., and Modi, D. (2020). Single-cell RNA-seq identifies cell subsets in human placenta that highly expresses factors driving pathogenesis of SARS-CoV-2. Front. Cell Dev. Biol. *8*, 783. https://doi.org/10.3389/fcell.2020.00783.

HGGA, Volume *3*

Supplemental information

X chromosome inactivation in the human placenta is patchy and distinct from adult tissues

Tanya N. Phung, Kimberly C. Olney, Brendan J. Pinto, Michelle Silasi, Lauren Perley, Jane O'Bryan, Harvey J. Kliman, and Melissa A. Wilson

Table of Contents

Supplementary Tables

Table S1. Number of heterozygous variants on the X chromosome and chromosome 8

For each sample, we reported the number of heterozygous variants after variant genotyping using GATK and after filtering using VQSR.

SampleID	X chromosome	Chromosome 8
OBG0044	951	1691
OBG0068	1468	2218
OBG0111	832	1650
OBG0115	964	1568
OBG0120	824	1674
OBG0133	1316	2134
OBG0156	997	1600
OBG0170	1390	1979
OBG0174	1426	2158
OBG0175	607	1594
OBG0178	1157	1906
OBG0166	804	1620
OBG0022	1125	1964
OBG0024	1206	2152
OBG0026	1907	2912
OBG0028	1706	2730
OBG0030	1842	3126
OBG0039	1086	2359
OBG0050	1786	2553
OBG0051	1107	2154
OBG0066	2010	2906
OBG0121	1805	2747
OBG0138	1044	2268
OBG0180	1110	2257
OBG0188	1940	2874
OBG0201	1757	2741
OBG0205	1275	2393
OBG0289	2020	2805
OBG0338	1049	2093
OBG0342	1169	2139

Table S2. Mapped reads at each extraction site for the whole transcriptome and for the X chromosome.

For each sample, we used samtools stats to obtain the number of reads that mapped.

Sample ID	Site A		Site B	
	Whole transcriptome	Chr X	Whole transcriptome	Chr X
OBG0044	124821361	2570404	104951941	1956346
OBG0068	96468961	2028381	72630017	1632320
OBG0111	105360653	2210820	87310785	1746585
OBG0115	115047845	2233186	81406062	1794380
OBG0120	109637796	2360408	78369660	1653373
OBG0133	106542634	2158139	75940154	1709600
OBG0156	123238340	2617278	79648267	1954931
OBG0170	104502826	2539731	101090503	2263802
OBG0174	29178948	589785	95550124	1787220
OBG0175	98337411	2134510	85986263	2061137
OBG0178	114938081	2447404	86675194	1916321
OBG0166	114474479	2532057	93337543	2043997
OBG0022	79624620	1846538	77386563	2048223
OBG0024	56525905	1464827	136862205	3467075
OBG0026	59648434	1014174	86201051	1772717
OBG0028	69962192	1894168	42201549	964035
OBG0030	75533477	1797735	72423761	1799896
OBG0039	81923032	1986227	60580683	1631386
OBG0050	72749515	1711200	62546230	1564591
OBG0051	78292464	1885179	61467811	1513737
OBG0066	74368314	1535224	80264229	2054109
OBG0121	95299259	2477900	40005508	1132595
OBG0138	217429809	5692793	73761980	1578129
OBG0180	72664680	1974885	29697974	837063
OBG0188	21675595	617351	79407643	2295587
OBG0201	88301001	2190583	80598634	2085968
OBG0205	49073152	1316484	40796256	1070053
OBG0289	72176230	1850324	78471721	1954236
OBG0338	75400996	1972344	57209598	1381726
OBG0342	80308862	1916568	85785465	2074156

Table S3. Number of heterozygous and expressed variants on the non-pseudoautosomal regions of the X chromosome and chromosome 8

After running GATK ASEReadCounter, we tabulated the number of heterozygous variants that are expressed (where total RNA read count is greater than 10).

Sample ID	Chromosome X		Chromosome 8	
	Site A	Site B	Site A	Site B
OBG0044	97	87	219	214
OBG0068	100	94	251	258
OBG0111	74	65	170	161
OBG0115	76	68	166	151
OBG0120	74	57	241	197
OBG0133	103	94	239	211
OBG0156	100	93	218	222
OBG0170	120	124	270	268
OBG0174	62	120	116	239
OBG0175	61	87	167	182
OBG0178	89	87	223	219
OBG0166	89	67	193	176
OBG0022	119	112	234	244
OBG0024	100	212	177	344
OBG0026	109	125	262	273
OBG0028	92	159	153	253
OBG0030	165	168	362	373
OBG0039	68	94	225	297
OBG0050	160	148	256	274
OBG0051	100	91	249	214
OBG0066	160	127	422	355
OBG0121	186	95	338	176
OBG0138	191	77	534	212
OBG0180	92	43	262	133
OBG0188	59	183	111	336
OBG0201	125	131	304	328
OBG0205	71	61	169	144
OBG0289	161	171	319	316
OBG0338	87	63	244	173
OBG0342	92	96	255	288

Table S4. Number of samples for each adult GTEx tissue.

The number of samples for each adult GTEx tissue used in this study (column 2), and the number of skewed samples (median allele balance greater than 0.8) (column 3).

GTEx tissues	Number of samples	Number of skewed samples
Adipose_Subcutaneous	194	19
Adipose_Visceral_Omentum	149	11
Adrenal_Gland	94	18
Artery_Aorta	138	7
Artery_Coronary	84	11
Artery_Tibial	187	14
Brain_Amygdala	37	2
Brain_Anterior_cingulate_cortex_BA24	42	2
Brain_Caudate_basal_ganglia	52	3
Brain_Cerebellar_Hemisphere	51	5
Brain_Cerebellum	58	4
Brain_Cortex	64	4
Brain_Frontal_Cortex_BA9	48	2
Brain_Hippocampus	49	2
Brain_Hypothalamus	47	1
Brain_Nucleus_accumbens_basal_ganglia	55	4
Brain_Putamen_basal_ganglia	42	3
Brain_Spinal_cord_cervical_c-1	48	1
Brain_Substantia_nigra	33	2
Breast_Mammary_Tissue	151	20
Colon_Sigmoid	113	3
Colon_Transverse	136	15
Esophagus_Gastroesophageal_Junction	110	3
Esophagus_Mucosa	176	32
Esophagus_Muscularis	162	9
Heart_Atrial_Appendage	119	9
Heart_Left_Ventricle	122	21
Kidney_Cortex	18	0
Liver	62	12
Lung	166	13
Minor_Salivary_Gland	40	4
Muscle_Skeletal	237	17
Nerve_Tibial	177	13
Ovary	167	21
Pancreas	116	23
Pituitary	71	4
Skin_Not_Sun_Exposed_Suprapubic	169	28
Skin_Sun_Exposed_Lower_leg	208	35
Small_Intestine_Terminal_Ileum	63	5
Spleen	86	4
Stomach	122	15
Thyroid	196	14
Uterus	129	10
Vagina	141	20
Whole_Blood	229	60

Table S5. Number of heterozygous sites identified in nonPARs in XY males.

Sample	Number of called variants (AC > 0)	Number of heterozygous variants (AC = 1)	Number of heterozygous & expressed variants in site A	Number of heterozygous & expressed variant in site B
OBG0112	1,479	213	27	32
OBG0116	2,018	174	18	18
OBG0117	1,343	149	31	27
OBG0118	1,484	180	24	25
OBG0122	1,413	126	15	11
OBG0123	1,762	149	22	23
OBG0126	1,898	171	20	20
OBG0130	1,566	197	23	28
OBG0132	1,946	182	20	18
OBG0158	1,620	223	28	27
YPOPS0006	1,510	180	26	27
OBG0053	1,532	172	23	30

Table S6. Inactivation status for X chromosome genes in the placenta.

Inactivation status for X chromosome genes in the placenta assigned to criteria outlined in Supplemental Note 1 (in alphabetical order). Columns are defined as Gene (Gene Name of 198 X chromosome genes), Category (calculations for which category proportions are being calculated; either inactivated or escape), N Samples (number of samples fitting this category), N Total (total number of samples examined), Prop (proportion of the total samples fitting this category), and Gene Status (conclusion reached for this gene outlined in Supplemental Note 1).

Found in the accompanied Excel spreadsheet: "TableS6.xlsx"

Table S7. Paternal X chromosome is preferentially silenced.

The fourth column denotes the number of heterozygous and expressed variants that are skewed (allele balance ≥ 0.8 or ≤ 0.2). The fifth column denotes the number of variants that are heterozygous, expressed, and skewed in the placenta samples but are homozygous in the decidua samples. The sixth column denotes the number of variants where the biased allele from the placenta samples is the same as the decidua samples, which suggest that the biased allele is maternal in origin. The last column is our best guess of whether the maternal or the paternal X is silenced. If most of the heterozygous, expressed, and skewed variants are maternal in origin, we determined that the maternal X is active and the paternal X is silenced. For each placenta sample where the number of variants that are heterozygous in the placenta and homozygous in the decidua is less than or equal to 3 is also annotated uncertain.

Category	Sample	Site	Heterozygous, skewed, expressed, variants	Homozygous decidua variants	Matched biased allele in decidua & placenta	Maternal/Paternal silenced
Both sites are skewed towards the same haplotype	OBG0338	A/B	43	16	15	Paternal
		B	31	12	12	Paternal
	OBG0342	A	47	2	2	Paternal/Uncertain
		B	63	3	2	Paternal/Uncertain
	OBG0024	A	53	5	5	Paternal
		B	120	10	10	Paternal
	OBG0188	A	25	0	0	Unknown
		B	92	5	4	Paternal
	OBG0030	A	93	45	45	Paternal
		B	72	35	35	Paternal
	OBG0205	A	22	3	2	Paternal/Uncertain
		B	28	3	2	Paternal/Uncertain
	OBG0289	A	69	3	1	Paternal/Uncertain
		B	89	3	2	Paternal/Uncertain
	OBG0026	A	33	0	0	Unknown
		B	50	0	0	Unknown
Site A is skewed towards haplotype 1 but site B is biallelic	OBG0066	A	66	6	6	Paternal
		B	12	1	1	Paternal/Uncertain
	OBG0051	A	68	5	5	Paternal
		B	9	3	3	Paternal/Uncertain
	OBG0039	A	46	2	2	Paternal/Uncertain
		B	5	0	0	Unknown
Both sites are skewed towards opposite haplotypes	OBG0121	A	99	11	0	Maternal
		B	31	8	8	Paternal
	OBG0022	A	48	21	4	Maternal
		B	29	15	15	Paternal
	OBG0050	A	75	12	12	Paternal
		B	51	8	0	Maternal
	OBG0138	A	114	13	11	Paternal
		B	37	3	2	Paternal/Uncertain
	OBG0201	A	79	4	0	Maternal
		B	60	1	1	Paternal/Uncertain
	OBG0028	A	66	4	2	Uncertain
		B	46	2	2	Paternal/Uncertain
	OBG0180	A	39	15	4	Maternal
		B	19	4	4	Paternal

Supplementary Figures

Figure S1. Whole exome post-trimming FastQC Mean Quality Scores.

We used fastQC to check for quality of reads after trimming and used multiQC to aggregate results (A) 12 placenta samples from batch 1. (B) 18 placenta samples from batch 2.

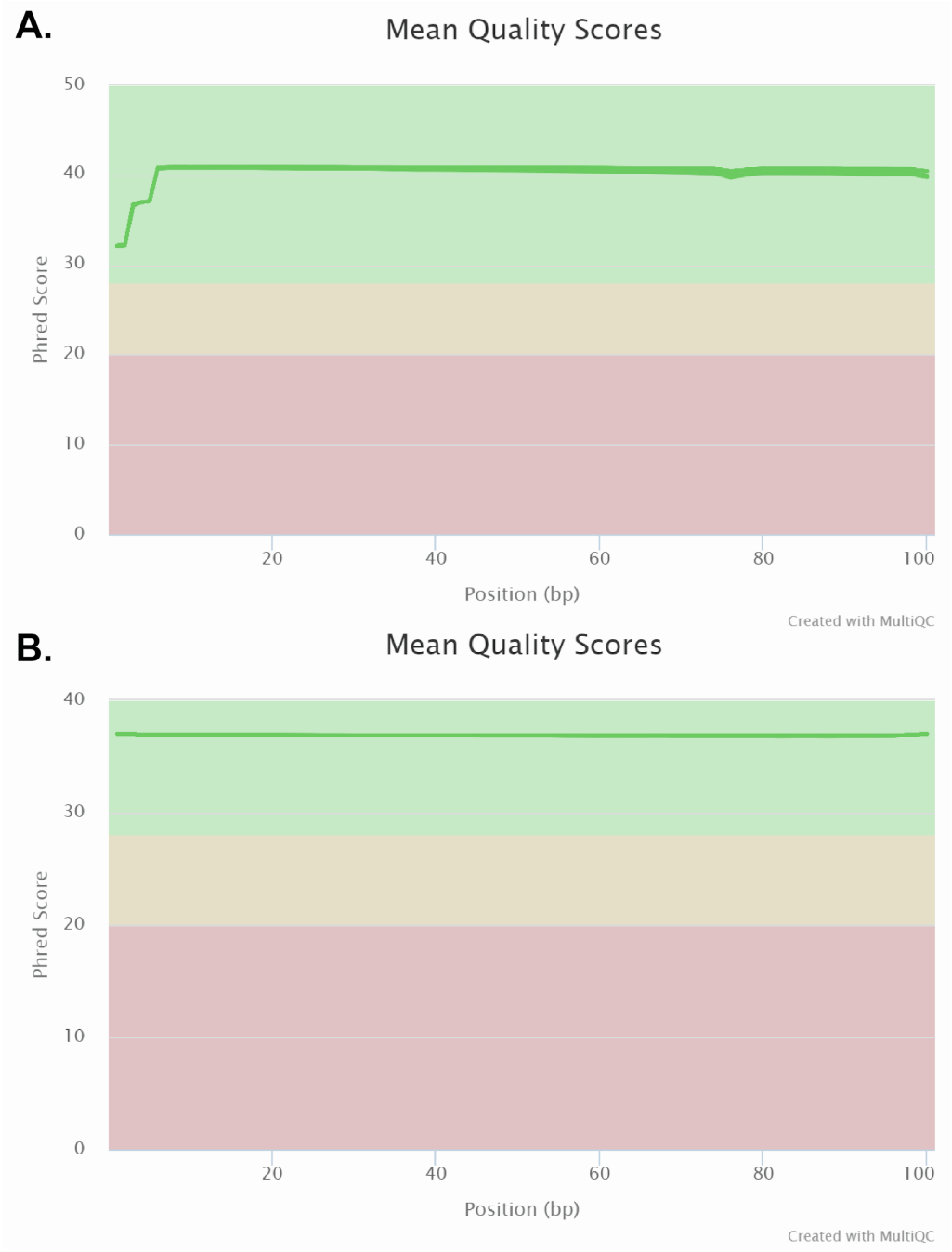

Figure S2. Reads mapped ratio.

The number of reads mapped to the X chromosome, the Y chromosome, and chromosome 19 was obtained by running samtools stats. Ratios in reads mapped were plotted for between the X chromosome and chromosome 19 (chrX/chr19), between the Y chromosome and chromosome 19 (chrY/chr19), and between the Y chromosome and the X chromosome (chrY/chrX). We observed that the ratio of reads mapped ratio between the X chromosome and chromosome 19 is much lower for OBG0175 than all other samples, suggesting that this sample is not genetic XX sample. Therefore, we removed this sample from further analyses.

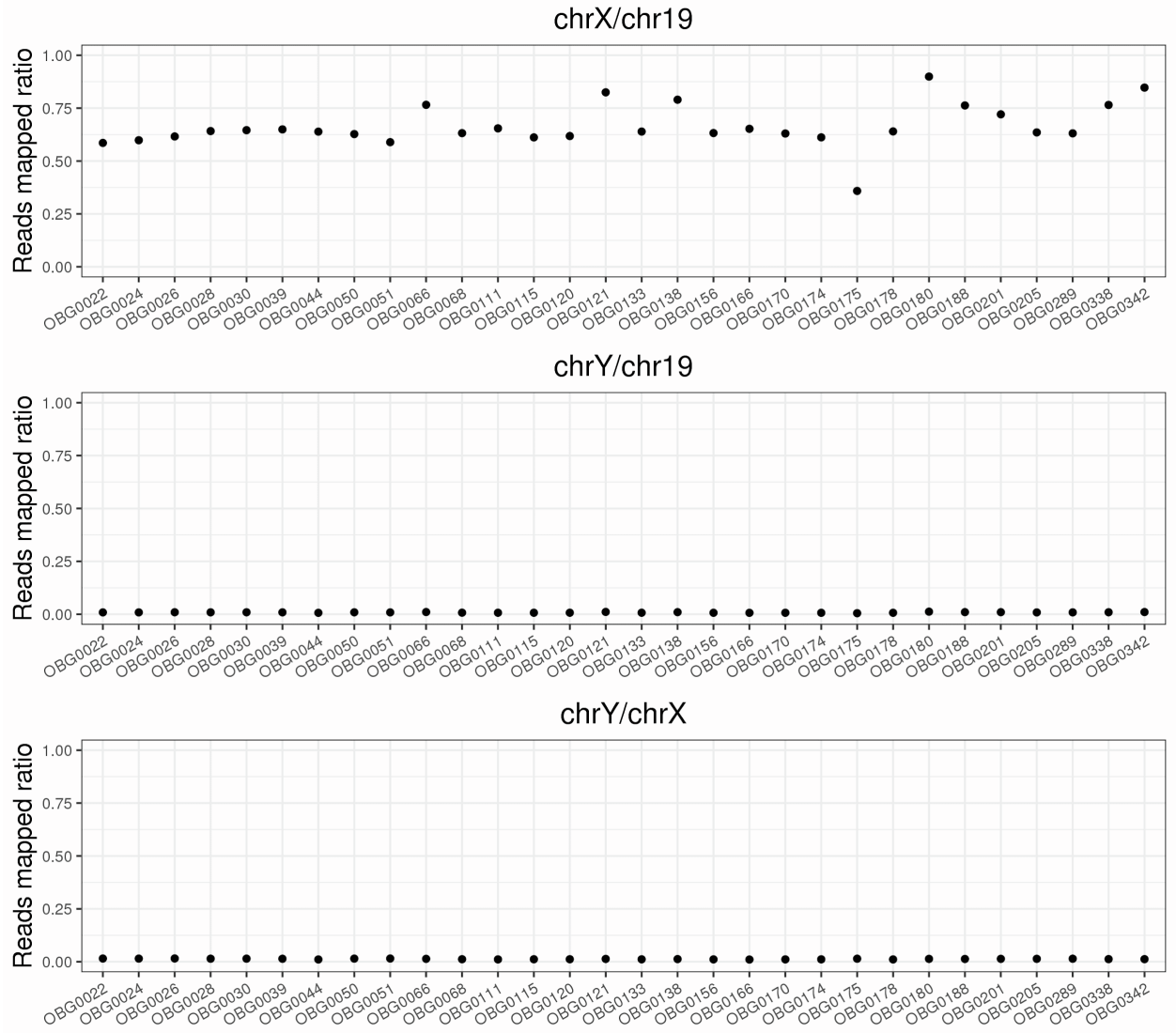

Figure S3. Principal component analysis for placenta samples.

Principal component for principal component 1 and 2 for the X chromosome (left panel) and for chromosome 8 (right panel) using the exome data from batch 1 and batch 2. We observed no clear separation by batches between these samples. The batch 1 samples are: OBG0044, OBG0068, OBG0111, OBG0115, OBG0120, OBG0133, OBG0156, OBG0170, OBG0174, OBG0175, OBG0178, and OBG0166. The batch 2 samples are: OBG0022, OBG0024, OBG0026, OBG0028, OBG0030, OBG0039, OBG0050, OBG0051, OBG0066, OBG0121, OBG0138, OBG0180, OBG0188, OBG0201, OBG0205, OBG0289, OBG0338, and OBG0342.

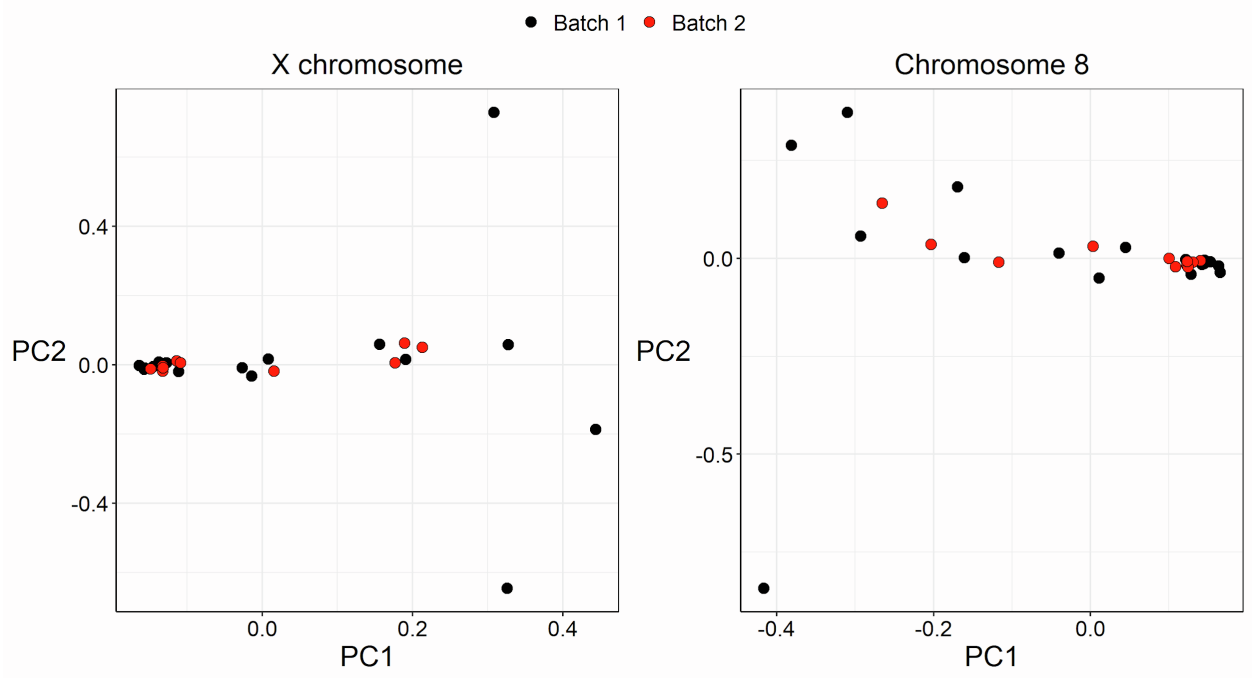

Figure S4. Whole transcriptome post-trimming FastQC Mean Quality Scores.

We used fastQC to check for quality of reads after trimming and used multiQC to aggregate results (A) 12 placenta samples from batch 1. (B) 18 placenta samples from batch 2.

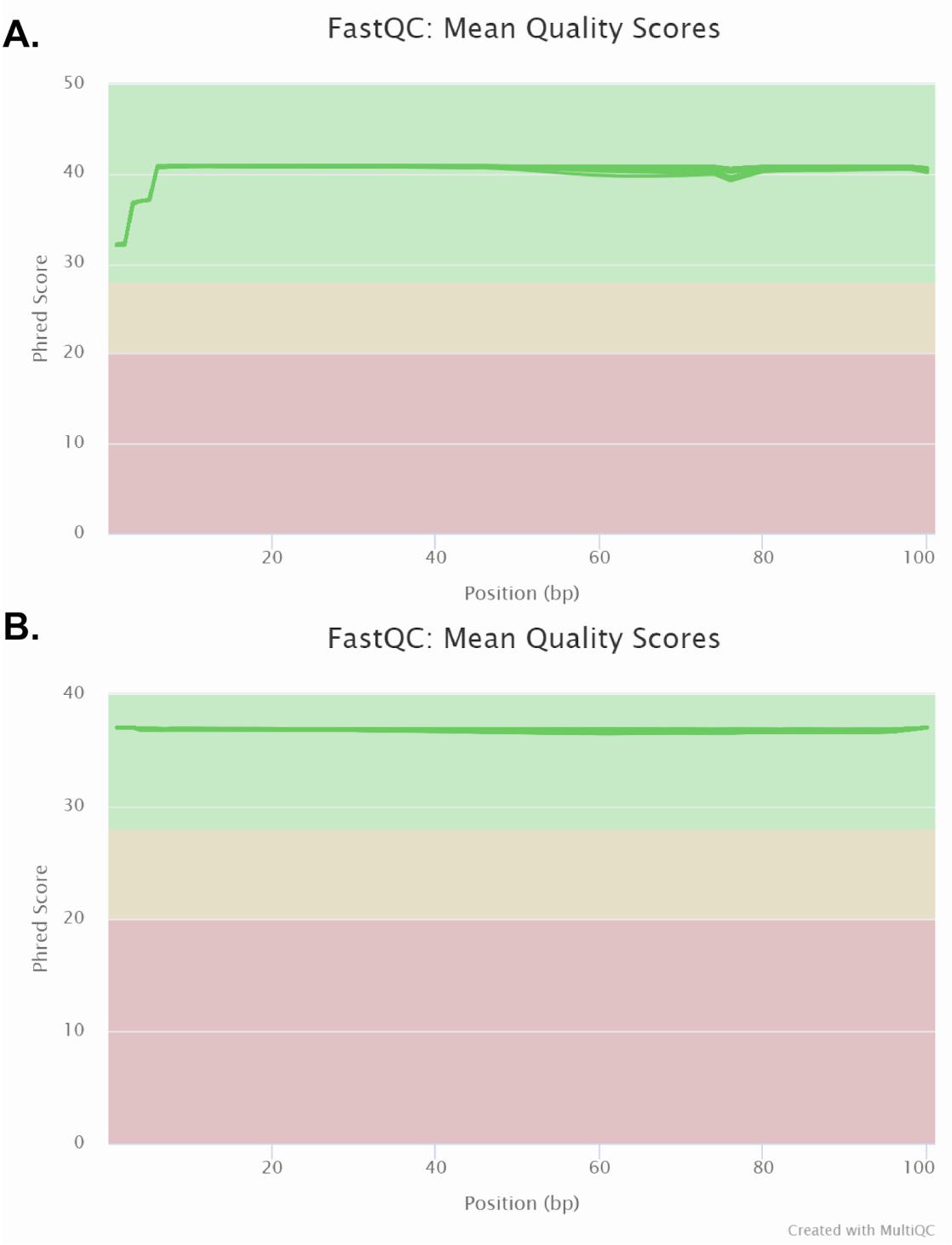

Figure S5. Determining threshold for skewed inactivation.

Each plot is a histogram of the allele balance for chromosome 8 (gray bars) and the X chromosome (yellow bars) for site A (left) and site B (right). Dotted lines denote allele balance of 0.8. We observed that the allele balance of most variants on chromosome 8 is less than 0.8 while the allele balance of most variants on the X chromosome is greater than 0.8.

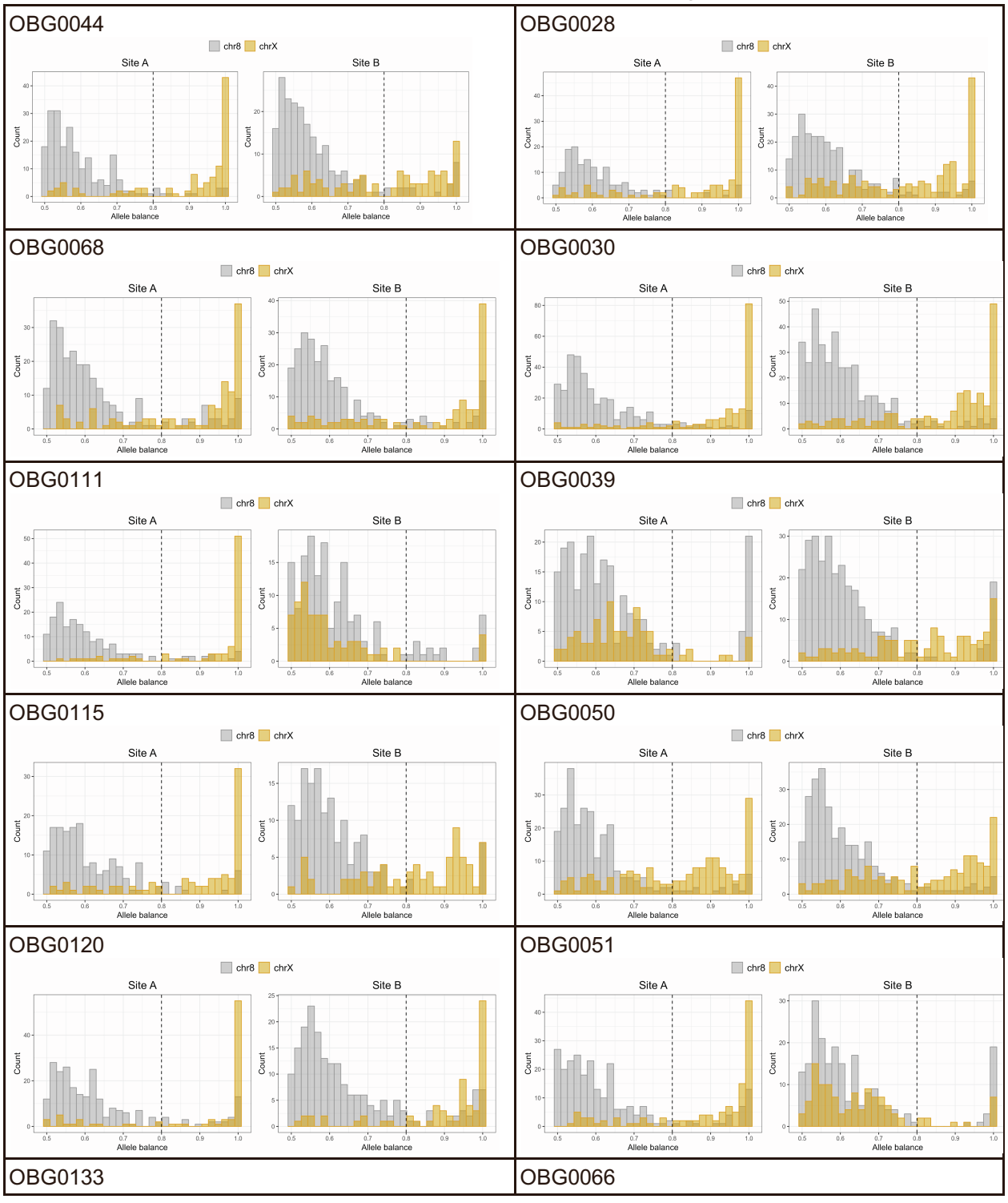

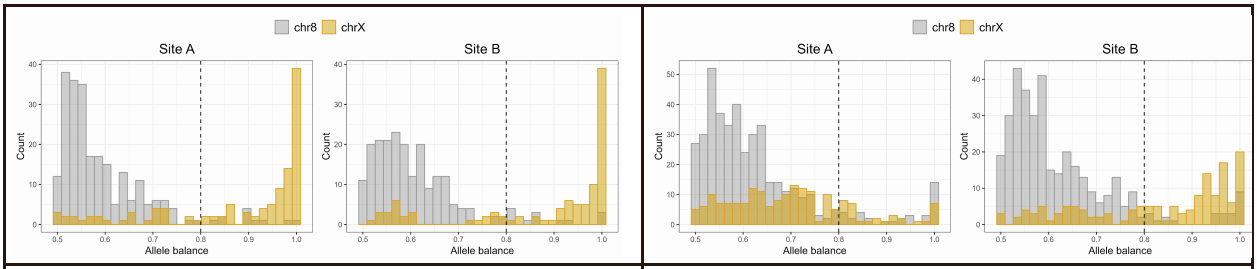

OBG0156

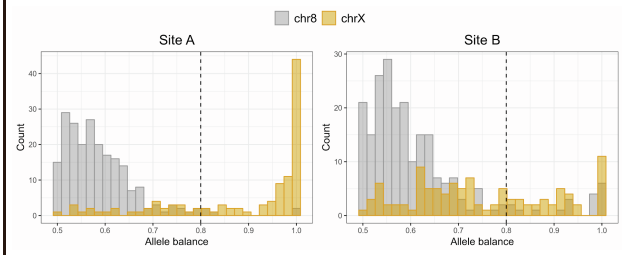

OBG0121

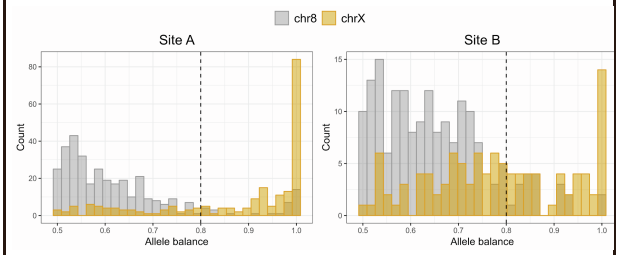

OBG0170

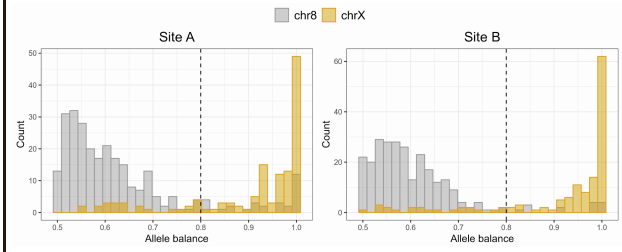

OBG0138

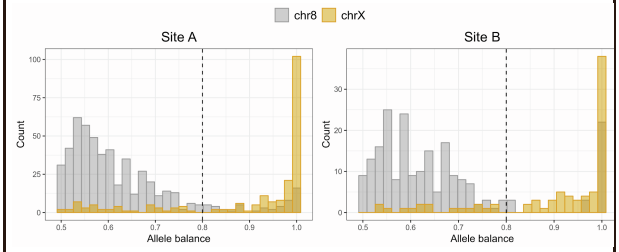

OBG0174

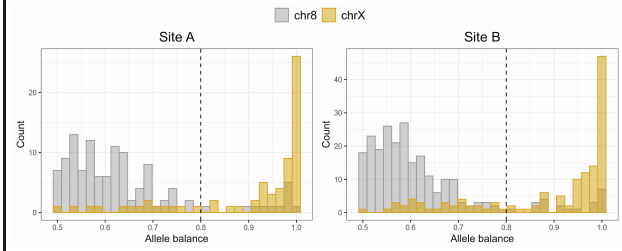

OBG0180

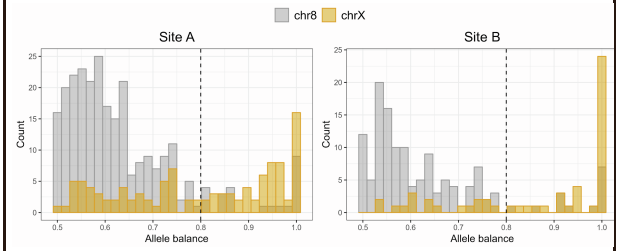

OBG0175

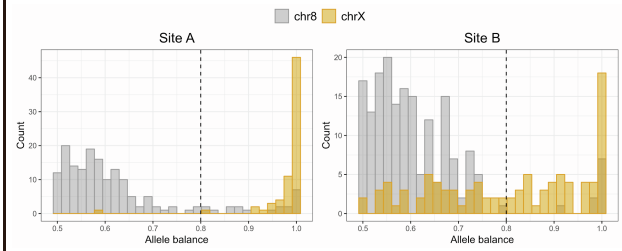

OBG0188

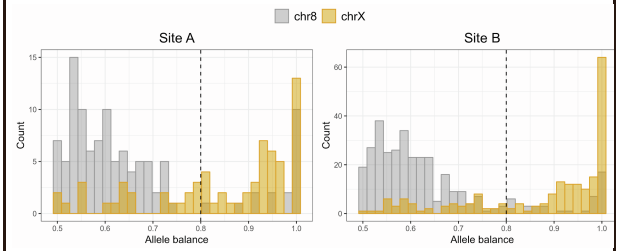

OBG0178

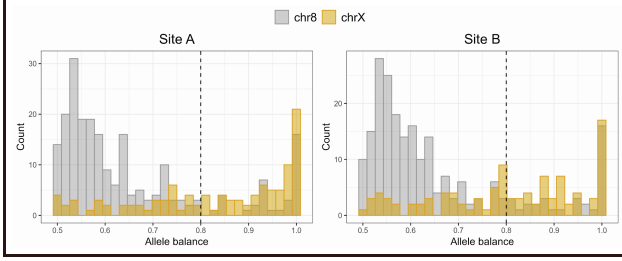

OBG0201

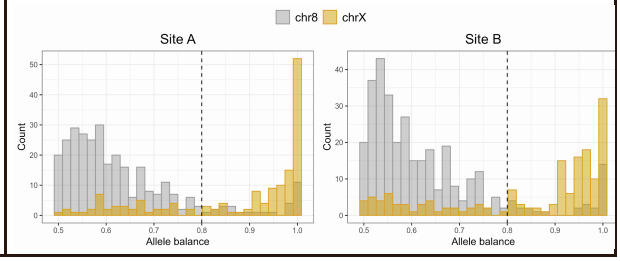

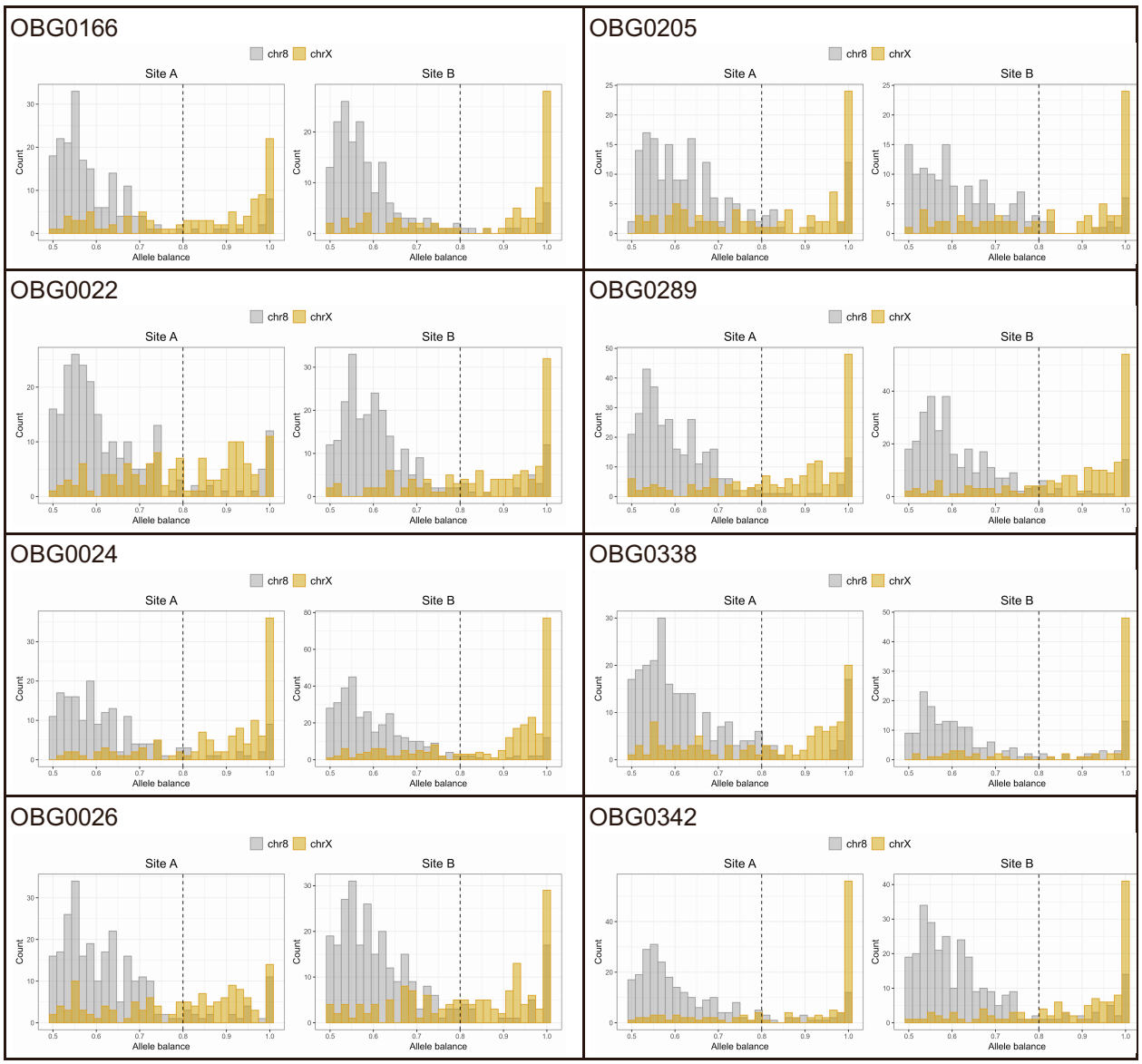
OBG0166
OBG0205
OBG0022
OBG0289
OBG0024
OBG0338
OBG0026
OBG0342
chr8
chrX
Site A
Site B
Count
Allele balance

Figure S6. Most variants of chrX non-PARs in XY males are skewed.

Histogram of allele balance in nonPARs in male XY samples called as diploid. We joint-called genotypes on 12 XY placentas (see **Methods**). Expression of variants on the nonPARs of the X chromosome should be completely biased towards one allele because there is only one X chromosome. However, even if we called the nonPARs as diploid, we wrongly identified only a small number of variants to be heterozygous (**Table S5**).

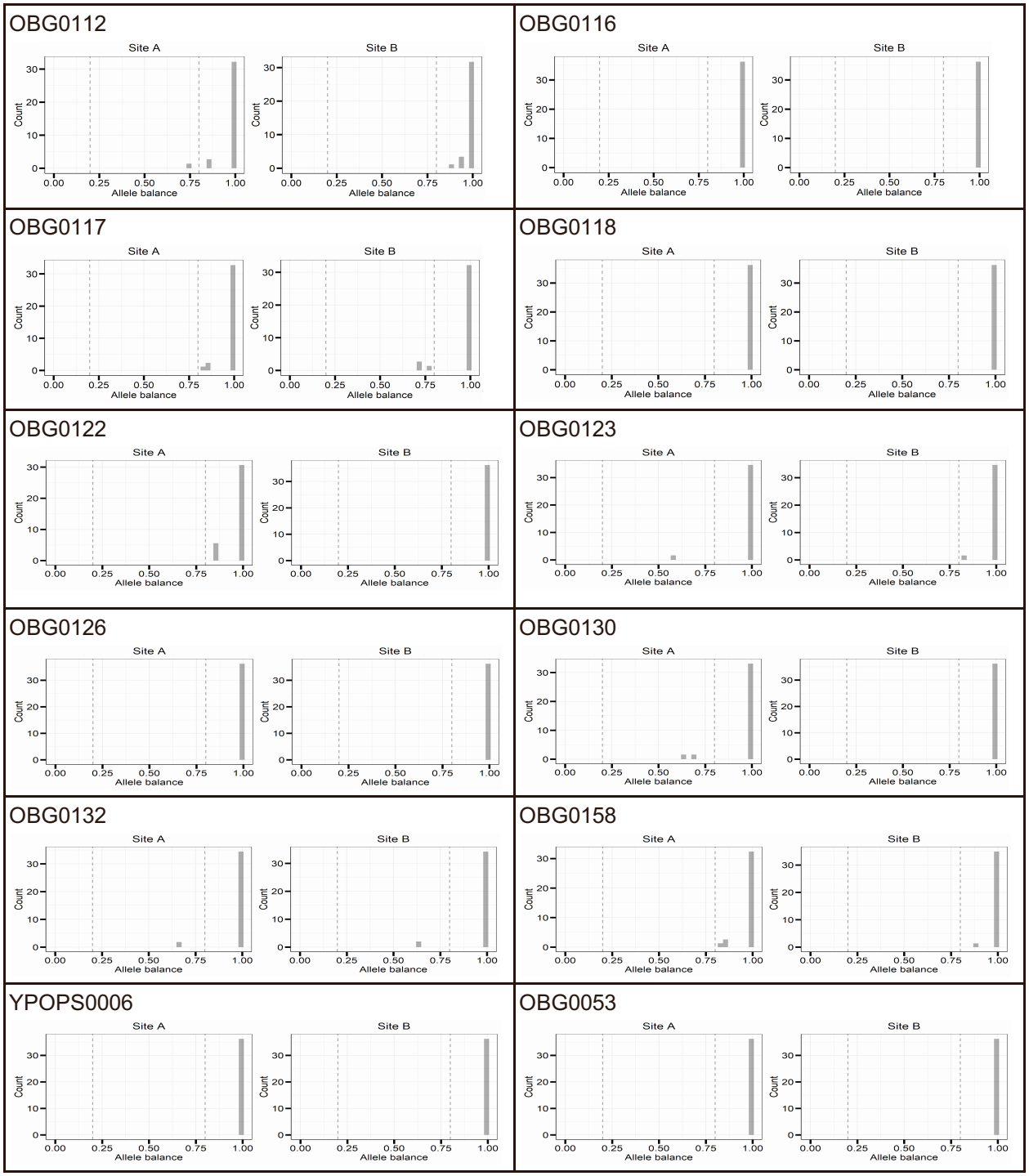

Figure S7. Patterns of X-inactivation across the entire X chromosome.

In each plot, allele balance at each heterozygous and expressed variant is plotted as a function of the position on the X chromosome. Open black circles denote variants on extraction site A. Filled red triangles denote variants on extraction site B. Gray boxes denote the pseudoautosomal regions and XIST.

A. Both extraction sites show the same X chromosome being inactivated

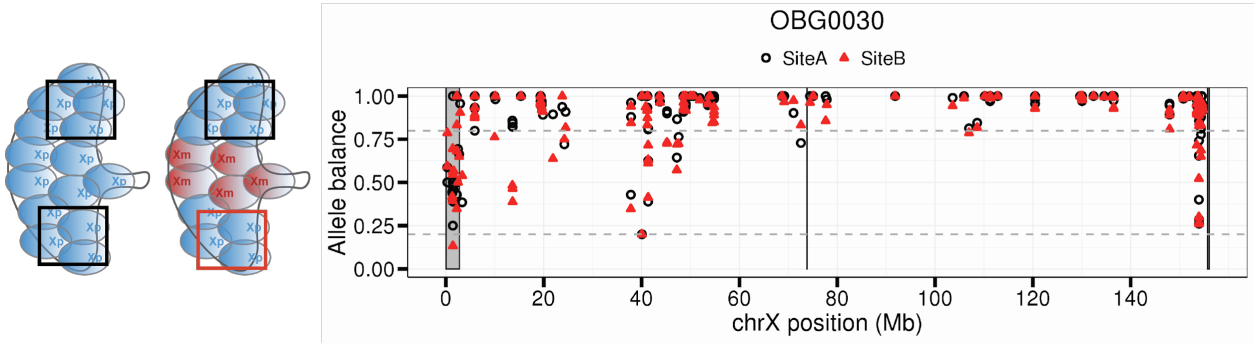

B. Each site shows a different X chromosome being inactivated

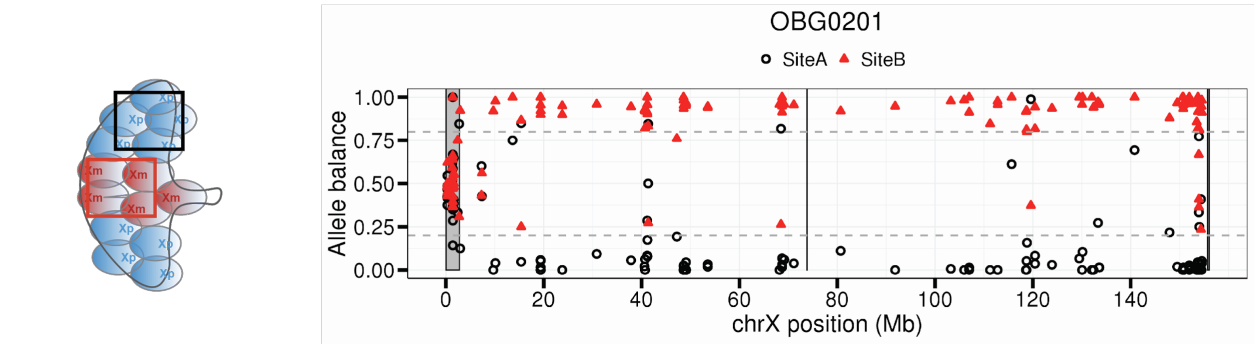

C. One extraction site shows skewed X-inactivation and the other shows both X chromosome being expressed

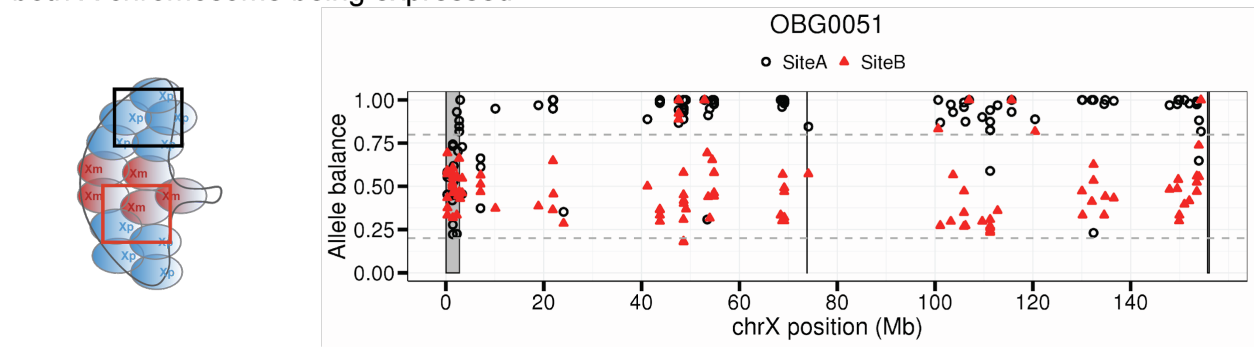

Figure S8. Chromosome 8 shows biallelic expression in placenta and adult tissues.

Unphased median allele balance is plotted for the placenta in this study (purple) and for 45 adult tissues in the GTEx dataset (blue) on chromosome 8. Each point of the violin plot is the median allele balance for each sample. Because there are no multiple site samplings for the GTEx data, unphased allele balance was computed.

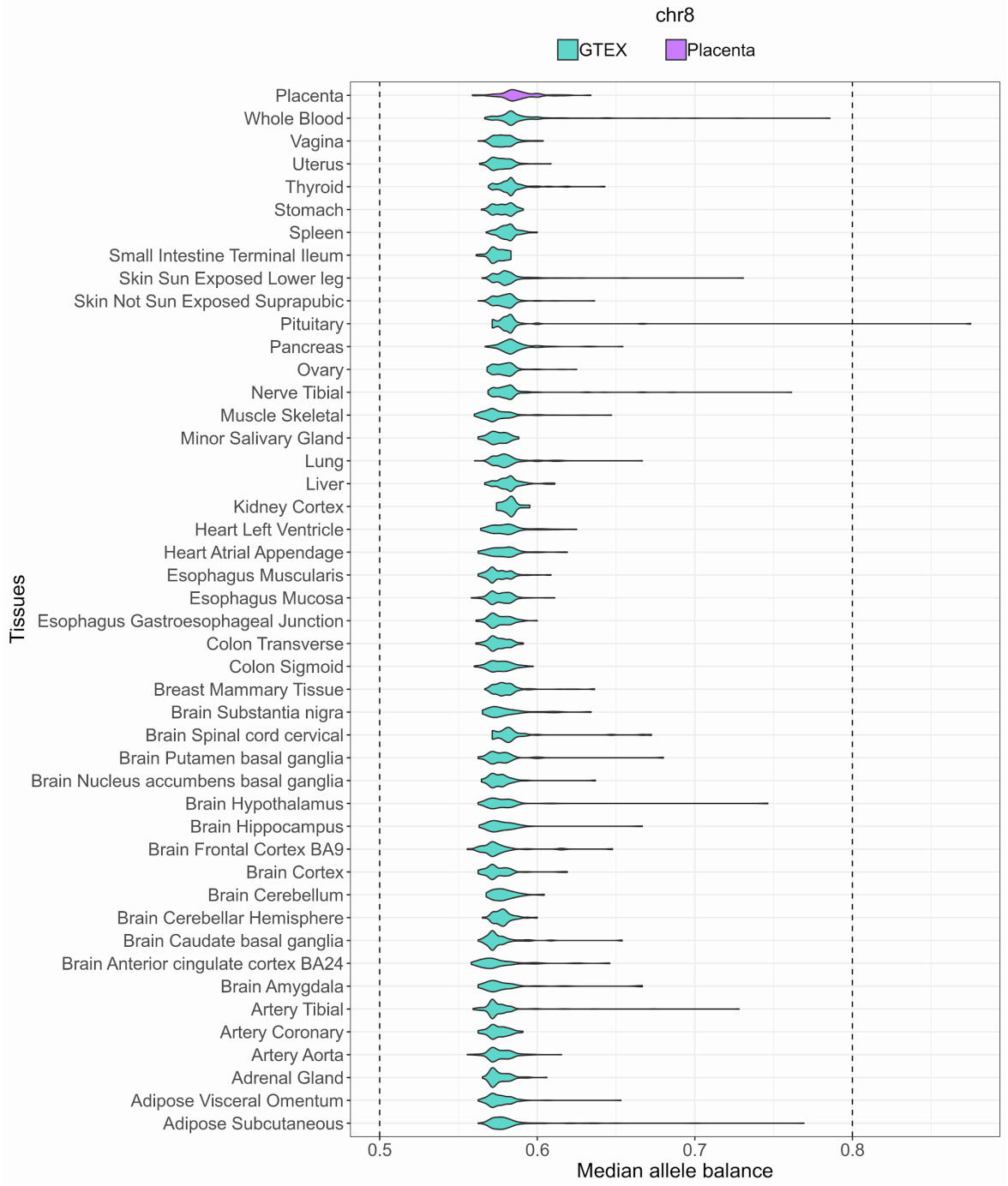

Figure S9. Heterogeneity in proportion of samples per gene that escape X-inactivation or are silenced.

For each gene, the dark blue bar denotes the proportion of samples that show evidence for that gene escaping XCI. The yellow bar denotes the proportion of samples that show evidence for that gene being silenced.

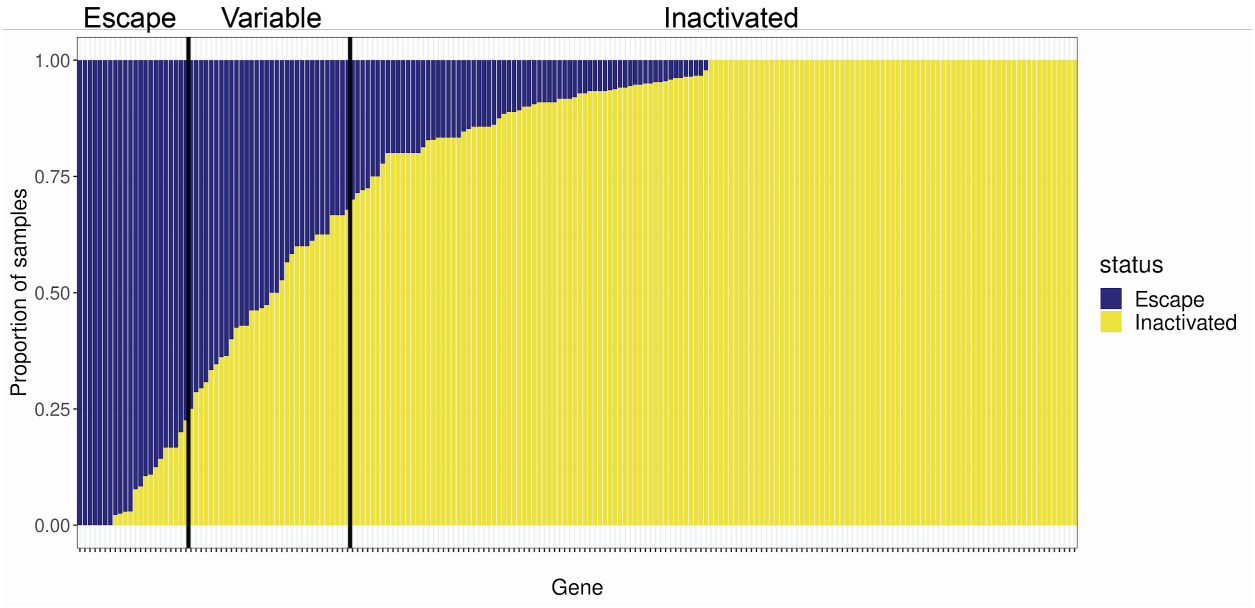

Figure S10. Heterogeneity in escape from X chromosome inactivation across and within placentas.

For each gene on the X chromosome, inactivation status is shown for each extraction site for each sample: dark blue (genes that escape XCI) and yellow (genes that are inactivated).

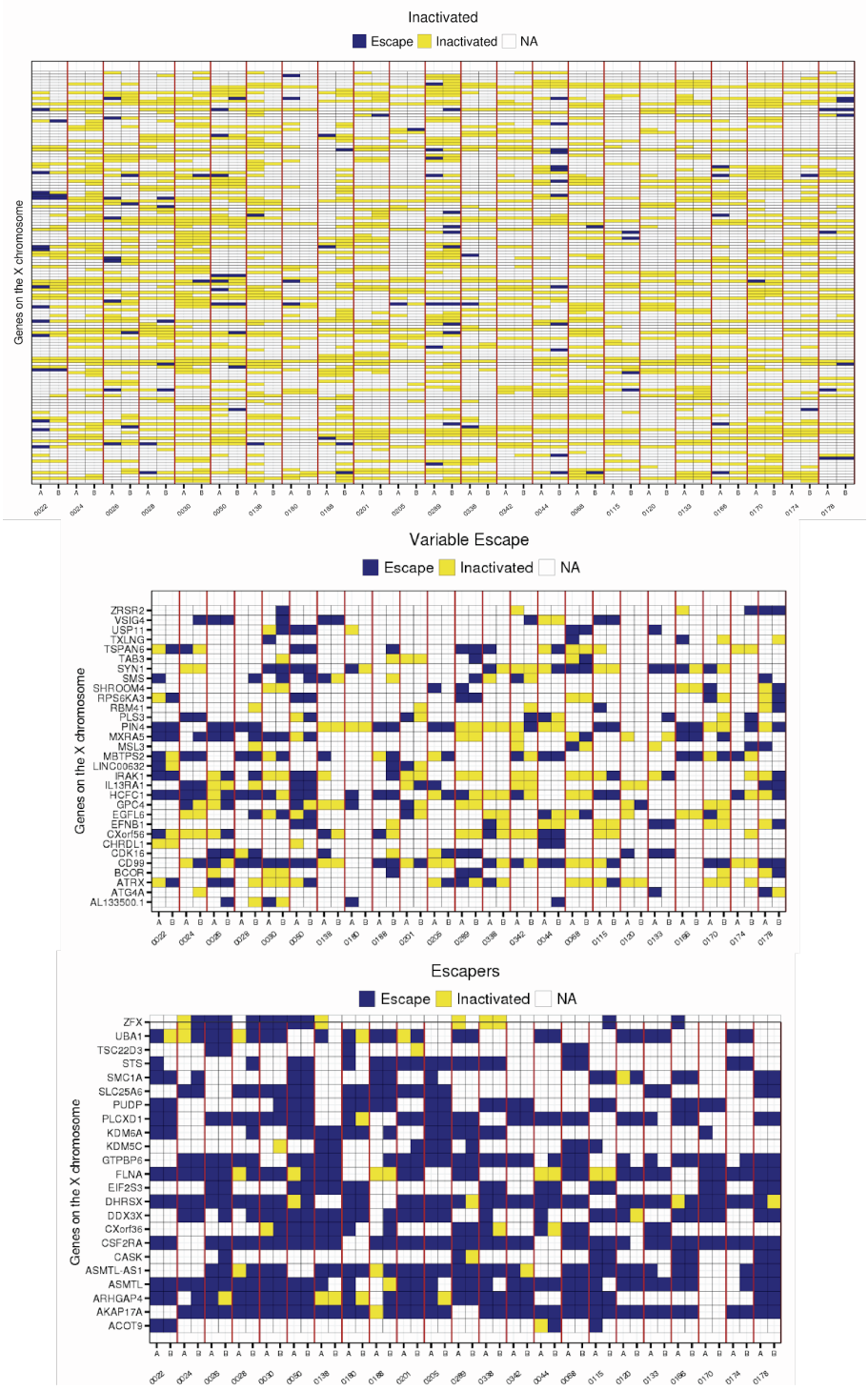

Figure S11. Higher gene expression in female does not necessarily equate to escape gene

Female to male $\log_2$ ratio (calculated as $\log_2(\text{female}_{CPM}/\text{male}_{CPM})$ in gene expression was computed for genes categorized as inactivated, escape, or variable in the placenta. The female_{CPM} and male_{CPM} were obtained from Olney et al. (unpublished data).

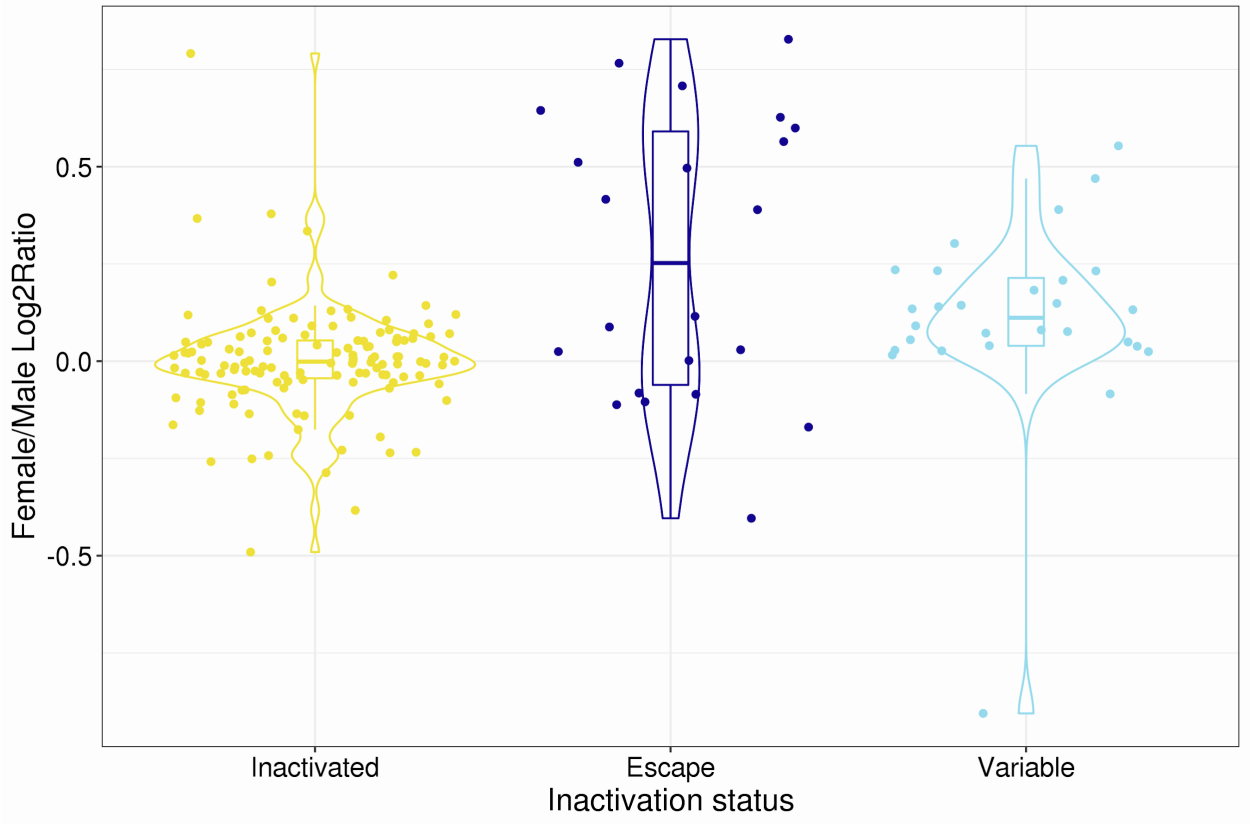

Figure S12. Total count and biased allele count for variants on genes that show opposite XCI patterns between the placenta and adult GTEx tissues and between the placenta.

For each gene, for each heterozygous and expressed variants, purple bars represent total RNA read count and light blue bars represent RNA read count of the biased allele. We observed that the total RNA read count for these variants are all greater than 10, suggesting that the patterns observed in Figure 4 is not due to technical artifacts.

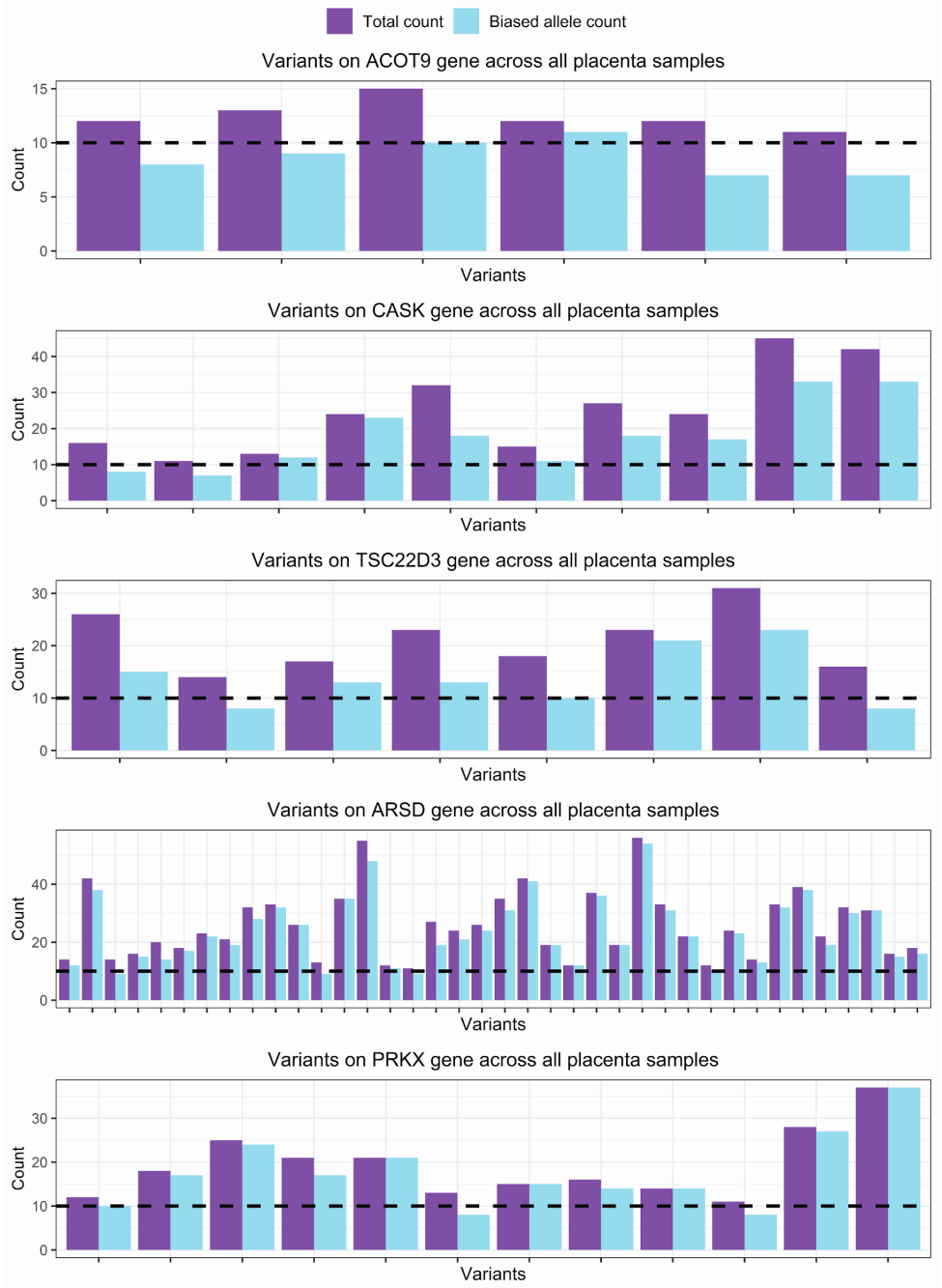

Supplementary Notes

Note 1. Method to classify genes into genes that are inactivated, genes that escape XCI, and genes that show variable escape